Hominin teeth from the Middle Pleistocene site of Yiyuan, Eastern China

Song Xing[a], Chengkai Sun[b, c*], María Martinón-Torres[d, e*], José María Bermúdez de Castro[d,f], Fei Han[g], Yingqi Zhang[a], Wu Liu[a]

a Key Laboratory of Vertebrate Evolution and Human Origins of Chinese Academy of Sciences, Institute of Vertebrate Paleontology and Paleoanthropology, Chinese Academy of Sciences, Beijing 100044, China
b Shandong Museum, Jinan 250014, China
c State Key Laboratory of Paleobiology and Stratigraphy, Nanjing Institute of Geology and Paleontology, Chinese Academy of Sciences, Nanjing 210008, China
d University College London (UCL) Anthropology, 14 Taviton Street, London WC1H 0BW, UK.
e Departamento de Ciencias Históricas y Geografía, Universidad de Burgos, Hospital del Rey s/n 09001 Burgos, Spain.
f Centro Nacional de Investigación sobre la Evolución Humana (CENIEH), Paseo de la Sierra de Atapuerca s/n, 09002 Burgos, Spain
g State Key Laboratory of Earthquake Dynamics, Institute of Geology, China Earthquake Administration, Beijing 100029, China
[*] Corresponding authors.
E-mail address: sunchengk@126.com (C. Sun) and maria.martinon.torres@gmail.com (M. Martinón-Torres)

Abstract

In 1981-1982, some hominin fossils, including a relatively complete skull and seven isolated teeth, were recovered from the Middle Pleistocene site of Yiyuan in Eastern China. In the present study we provide a detailed metric and morphological comparison of the Yiyuan dental sample in order to characterize the variability of the human populations that inhabited China during the Middle Pleistocene better. Aside from taxonomic and phylogenetic questions, the lack of understanding and/or knowledge about the morphological variability of these populations have caused concern about the human versus non-human nature of some of the hominin dental remains found in East Asia during the Early and the Middle Pleistocene. Thus, our study aims to present a detailed description and comparison of the Yiyuan isolated teeth to 1) discuss and support their human nature and 2) to explore their taxonomic affinities with regard to other penecontemporaneous populations from Asia. Our results clearly differentiate the Yiyuan sample from *Pongo* specimens and support a human attribution for the Yiyuan material. Our analyses also suggest that the Yiyuan teeth form a morphologically coherent group together with samples from Zhoukoudian, Chaoxian and Hexian. They are different from the more derived specimens from Panxian Dadong, suggesting a pattern of biogeographic isolation and different evolutionary trends between northern and southern China during the Middle Pleistocene. In addition, and despite sharing a common morphological bauplan with *Homo erectus* sensu stricto (s.s.), the Yiyuan, Zhoukoudian and Hexian teeth are also different from the Indonesian Early Pleistocene samples. In particular, the expression of a highly crenulated or dendritic enamel-dentine surface could be unique to these groups. Our study supports the notion that the taxonomy of the Pleistocene hominins from Asia may have been oversimplified. Futures studies should explore the variability of the Asian specimens and reconsider whether all the samples can be attributed to *H. erectus* s.s.

Introduction

Field seasons during 1981 and 1982 at the Yiyuan site, eastern China, yielded a nearly complete skull and seven isolated teeth. These human fossils were previously described by Lu et al. (1989) and assigned to *Homo erectus*, mainly because the skull displays typical features already described in the Zhoukoudian hominins, namely the marked frontal recession, postorbital constriction, deep postorbital sulcus, and strong superaorbital torus (Lu et al., 1989; Wu and Poirier, 1995). The associated mammal assemblage at Yiyuan was also similar to that found at Zhoukoudian Locality 1. However, some scholars (Wu et al., 1999) suggested that the Yiyuan hominins might represent a form of archaic *Homo sapiens*, mainly due to the absence of a cingulum in the teeth, which was thought to be a typical feature in Zhoukoudian *H. erectus*. Zhang and Liu (2002) carried out metrical and morphological comparisons between Chinese *H. erectus* and archaic *H. sapiens*. They pointed out that tooth crown

size was not useful to distinguish between these two groups, except for the buccolingual dimension of the upper central incisor. In addition, they stated that the primitive dental morphology displayed by *H. erectus* could also be found in archaic *H. sapiens*. In conclusion, Zhang and Liu (2002) proposed that *H. erectus* and archaic *H. sapiens* could be differentiated only at sub-species level and therefore, the Yiyuan hominins did not necessarily belong to *H. erectus*. Sun et al. (2011) specifically quantified the shape of the crown outline and occlusal polygon (i.e., the area formed by connecting cuspal apices, anterior and posterior foveae in upper premolars, see Gómez-Robles et al. [2011]) of the Yiyuan premolars and molars. This geometric morphometric study found that Chinese *H. erectus* and archaic *H. sapiens* had some morphological features in common, and that the Yiyuan hominins were less primitive than Chinese Early Pleistocene specimens.

Apart from these preliminary reports and comparisons, no systematic study of dental morphology and metrics has been made on the Yiyuan hominins. Furthermore, since discovery of the Yiyuan fossil hominins, the fossil record from the Early and Middle Pleistocene around the world has significantly increased (e.g. Wood, 1991; Tobias, 1991; Bermúdez de Castro et al., 1997; Gabunia et al., 2000), providing a much wider context to understand the morphological variability of this assemblage. Recent dental studies have also outlined clear dental evolutionary trends (Bailey, 2002, 2004; Gómez-Robles et al., 2007, 2008, 2011; Martinón-Torres et al., 2006, 2007, 2008, 2012; Zanolli, 2013), which allow more comprehensive investigation of the taxonomic affinities of the Yiyuan teeth. In addition, the recent application of micro-computed tomography (micro-CT) to the study of dental material (e.g., Skinner, 2008, 2009; Zanolli et al., 2010; Bailey et al., 2011; Martínez de Pinillos et al., 2014; Martinón-Torres et al., 2014; Zanolli, 2014) has unveiled a new source of palaeobiological information.

Some scientists have expressed concern about the accuracy of assessing whether fossil dental remains found in East Asia are human or non-human. Previous studies have pointed out the difficulties of differentiating some Asian hominin teeth from those of *Pongo* (e.g., Tyler, 2003, 2004; Smith et al., 2009, 2011; Ciochon et al., 2010; Zanolli et al., 2012, 2015) due to their overlapping chronologies, as well as the similarities in some morphological and metrical features. Assessing affinities becomes more complicated when fossil samples from the Middle Pleistocene hominins are considered, because of their complex occlusal surfaces at both the enamel and the dentine surfaces (e.g., see the molars of Hexian hominins in Xing et al. [2014]). Thus, our study presents a detailed metric and morphological study of the Yiyuan isolated teeth with two aims: 1) to evaluate whether the Yiyuan fossils are human or non-human and 2) to explore the taxonomic and phylogenetic status of Yiyuan hominins with regard to other penecontemporaneous populations from Asia. Our study will contribute to better characterization and understanding of the variability of East Asian hominins during the Middle Pleistocene.

The Yiyuan site
Between September 1981 and May 1982, a fossil hominin skull, seven isolated teeth, and associated mammal fossils were found at Qizianshan Mountain (118°09'E, 36°12'N), Yiyuan County, Shandong Province, Eastern China (Wu and Poirier, 1995; Fig. 1). Thirteen mammal species have been identified, with the most abundant being *Ursus arctos*, *Equus sanmeniensis*, *Sus lydekkeri*, and *Megaloceros pachyosteus* (for more details see Lu et al. [1989]). No stone artifacts were found at the site. Qizianshan is at an altitude of 496 m, and is geologically dominated by Ordovician limestone. So far, eight localities have been excavated or investigated at this site, and Localities 1, 2, and 3 have been explored systematically. These three localities are at the east side of Qizianshan Mountain, next to the River Ciyu. They are distributed within an area of 80 m (north to south) and at approximately the same level (4.5 – 6.0 m) above the bed of the River Ciyu). Most of the mammal fossils and all hominin materials came from Locality 1 and 3, and the present study will focus on them.
[Insert Figure 1]
Locality 1 is a cave site and its current entrance was opened by road construction. The cave is 3.2 m high and maximally 2 m wide at the bottom (Fig. 1). The systematic excavation started from a 1.3 m x 1.3 m area and reached the bedrock. The deposit at the west end of the cave still remains. Locality 3 is a fissure site with its opening facing upwards (Fig. 1). Its north – south extent is 25 m and the east – west extent ranges from 0.25 to 0.75 m. The excavation focused on the 7 southernmost meters of Locality 3. The final excavation was 3.5 m deep, 0.7 m wide at the top, and 0.3 m wide at the bottom. The stratigraphic sequences for Localities 1 and 3 are illustrated and described in Figure 1. Lu et al.

(1989) proposed that there was a good correlation layer by layer between Localities 1 and 3. Aside from differences in the thickness or the color of the deposits, the main components of the corresponding layers are similar. All hominin fossils and most faunal remains were recovered from reddish brown or dark brown silty clay in Layer 3. Although a systematic faunal study has not been performed to date, the mammal taxa in the two localities are similar. Based on the similarities of the deposits, Lu et al. (1989) assumed that all the hominin fossils belonged to the same geological time. Combined electron spin resonance and uranium-series dating performed on three animal teeth from Locality 1 and six animal teeth from Locality 3 (all of them from the layers where hominins were found) revealed that hominin occupation of the two Yiyuan localities occurred about ~420 to 320 thousands of years before present (ka BP) (Han et al., 2015).

Materials and methods

Samples
The seven Yiyuan isolated teeth (Sh.y.003, 004, 005, 007, 008, 071, and 072) represent five dental classes, P_3, P_4, M_2, C_1, and M_2. According to the fitting of the interproximal wear facets and/or the degrees of occlusal wear, Sh.y.003, 004, 008, and 071 from Locality 3 were assigned to the same individual. Sh.y.003 is the antimere of Sh.y.004, and there is a good interproximal fit between Sh.y.004 and Sh.y.071. Sh.y.005 and Sh.y.007 were recovered from Locality 1 together with the skull. Their color and degree of occlusal wear indicated that they probably belonged to the same individual (Table 1, also see Sun et al. [2014]). The Sh.y.072 from Locality 3 has a similar color to the other four teeth from this site, but its heavier occlusal wear and smaller crown size (especially compared to Sh.y.008) suggest that Sh.y.072 might represent a third individual.
[Insert Table 1]
To be consistent with the aim of this study, the Yiyuan fossil hominins were mainly compared to those from East Asian Early and Middle Pleistocene hominins, as well as other fossils from the same continent or those grouped under the taxon *H. erectus* sensu lato. In addition, in order to understand the polarity of the observed features better, a wider *Homo* sample from Africa, Asia and Europe was considered, including recent modern human collections from Henan and Hubei Province (Central China) that range from the Neolithic to the time of the Qing Dynasty (Table 2).
Grouping of the comparative samples follows the same criteria employed in Liu et al. (2013) and Xing et al. (2014), mainly based on the geographic locations and geological ages of the samples, except for *H. sapiens* and Neanderthals that, on dental grounds, are generally well recognized groups. For a detailed list see Table 2.

In order to support the human nature of the Yiyuan teeth and to emphasize their differences from *Pongo* teeth, up to 144 teeth belonging to fossil *Pongo* (Table 2) were added as a comparative sample in some of the analyses. All fossil *Pongo* teeth used in this study are curated at the Institute of Vertebrate Paleontology and Paleoanthropology (IVPP), Beijing. Some of the fossil *Pongo* teeth were collected from Guangxi Zhuangzu Autonomous Region in 1956 and 1957. The precise chronological age of these teeth is unknown due to the lack of stratigraphic information. The rest were unearthed at Baxiandong, Daxin Heidong, and Sanhe Caves (Guangxi region) between 2009 and 2013. The depositional age of fossil *Pongo* at Daxin Heidong could be traced back to the Middle Pleistocene (380 – 310 ka according to Rink et al. [2008]). Paleomagnetic dating of the fossil-bearing strata in Sanhe Cave gives an age of approximately 1.2 millions of years ago (Ma) (Jin et al., 2008; Wang et al., 2014). No exact dates are available for the materials from Baxiandong. However, the composition of the fauna recovered from these sites indicates that the *Pongo* teeth could be Pleistocene in age.
[Insert Table 2]

Methods
Tooth wear stages were scored according to the standard proposed by Molnar (1971). The terms employed for the morphological descriptions and comparisons came from Weidenreich (1937), Bermúdez de Castro (1988), Turner et al. (1991), Scott and Turner (1997), and Martinón-Torres et al. (2008). Some of the non-metric features were scored following the Arizona State University Dental Anthropology System (ASUDAS) (Turner et al., 1991).
Mesiodistal (MD) and buccolingual (BL) dimensions of the crown were measured with a standard

sliding caliper and recorded to the nearest 0.1 mm following Wolpoff (1971).

Measurement of the relative cuspal area Each M_2 was photographed with its cemento-enamel junction parallel to the camera lens (Bailey, 2004). The area of each cusp was measured in each picture by tracing the outline and main occlusal grooves with ImageJ. If the main occlusal grooves were too worn to be identified, the specimens were eliminated from the study. When a main occlusal groove did not reach the crown margin, this groove was manually extended to intersect with the crown margin based on its orientation. Where necessary, interproximal wear was corrected based on wear extent and the orientation of the crown outline (Wood et al., 1983). Most of the M_2s had four cusps: paracone, protocone, metacone, and hypocone. However, when an accessory cusp (C5) was present, it was divided equally and added to the areas of the adjacent cusps (i.e., metacone and hypocone). All measurements were taken by the same person (X.S.). After each cusp was measured, the total crown base area (TCBA) was obtained by adding the cusp base areas. Relative cusp base area was calculated by dividing each individual cusp base area by the total crown base area.

Microcomputed tomography, enamel-dentine junction surface reconstruction, and measurement of relative dentine horn height of M_2 The Yiyuan teeth display different degrees of occlusal wear. In some cases, several morphological features at the outer enamel surface (OES) are lost. In order to maximize the morphological information, digital three-dimensional surface models of the enamel-dentine junction (EDJ) were reconstructed from the high-resolution micro-computed tomography (micro-CT) scan. Each tooth was scanned using a 225kV-µCT scanner (designed by the Institute of High Energy Physics, Chinese Academy of Sciences, and housed at the Institute of Vertebrate Paleontology and Paleoanthropology, Chinese Academy of Sciences) equipped with a 1.0-mm aluminum filter under settings of 120kV, 120uA, 0.5 rotation step, 360 degrees of rotation, 4 frames averaging (four times of scanning for each angle, and the four raw projections were coalesced). Isometric voxel size is 12.5 microns. Raw projections were converted into image stacks of raw file format (tomographic slices) with IVPP225kVCT_Recon. The image stacks were saved at a resolution of 2048 x 2048 pixels. The VGstudio Program was employed to remove the empty spaces from the image stack to reduce data size and to save the data as raw volumes, which were then imported into Mimics 16.0 to complete the segmentation of enamel and dentine and to visualize the EDJ surface. During the process of enamel/dentine segmentation, 3D Livewire tools (an interactive segmentation method by adding points along the object's boundary on multiple slices), single/multiple slices modification, and thresholding were employed.

[Insert Figure 2]

In addition, of particular relevance in assessing whether the Yiyuan sample was human, we calculated the relative dentine horn height (RDHH) of Sh.y.008 (M_2) and compared it to a wide sample of *Pongo* and *H. sapiens* specimens, as RDHH has been shown to be a useful taxonomic discriminator among a wide variety of extinct and extant primates (e.g., Olejniczak et al., 2008; Zanolli et al., 2015). A mesial sectional plane (Fig. 2) was prepared following Olejniczak (2006). First, a horizontal plane was defined by three dentine horn tips (paracone, metacone, and protocone). Then, we defined a sectional plane, perpendicular to the previous one that simultaneously cuts through the dentine horn tips of the paracone and the protocone. Based on the mesial sectional plane, we measured the RDHH of the paracone and the protocone of Yiyuan M_2 (Sh.y.008) following the protocol outlined by Olejniczak et al. (2008). As indicated in Figure 2, the RDHH was calculated as $Yx100/(X+Y)$, where X was the dentine horn height defined as the perpendicular distance from the dentine horn to the line parallel to the bi-cervical diameter and coursing through the lowest point of enamel in the mid-occlusal basin, and X+Y was the total height of the dentine crown measured as the perpendicular distance from the dentine horn to the bi-cervical diameter. The RDHHs of Sh.y.008 were compared to the values obtained in this study (10 *Pongo* and 48 recent modern humans), as well as the values for *Pongo* and *H. sapiens* from Olejniczak et al. (2008). In Olejniczak et al. (2008), all maxillary molars were combined to produce a mean RDHH because "the metameric variation in the molar row were unlikely to contribute to the overall variation within each taxon's RDHH" (Olejniczak et al., 2008, p. 89; see also Smith et al. [2005]). Therefore, the mean RDHH for all the maxillary molars is comparable to the RDHH of each tooth from the maxillary molar row.

Geometric morphometric (GM) analysis A Cannon EOS 5D digital camera equipped with a 100 mm lens was used to take a high resolution photo of each tooth with the plane formed by its cemento-enamel junction (CEJ) parallel to the camera lens (Martinón-Torres et al., 2006; Gómez-Robles et al., 2007, 2008, 2011). When both antimeres were present and equally well preserved in the comparative sample, only the same side as that represented at the Yiyuan site was

chosen. If only one antimere was preserved and happened to be from the opposite side to the one preserved at Yiyuan, the tooth was mirror-imaged using Adobe Photoshop®.

Geometric morphometrics allows shape variation among specimens to be analyzed quantitatively based on landmark and/or semi-landmark coordinate data (Adams et al., 2004; Zelditch et al., 2004). Landmarks are homologous anatomical points that could be defined repeatedly among specimens (Zelditch et al., 2004). Semi-landmarks are defined as "loci that have no anatomical identifiers but remain corresponding points in a sense satisfactory for subsequent morphometric interpretation" (Bookstein, 1999, p. 74). They can be used to examine the outline shape in lack of the real landmarks (Bookstein, 1997, 1999). During the GM analysis, non-shape elements such as position, size, and orientation will be eliminated through the processes of translation, scaling and rotation (superimposition) (Zelditch et al., 2004). Among the different ways of superimposition, we used generalized least squares or GLS method. GLS iteratively minimizes the difference in shapes or landmark configurations by maximally reducing the Procrustes distance (the square root of the sum of squared distances between the coordinates of corresponding landmarks) (Zelditch et al., 2004). Geometric morphometric analysis was carried out on standardized occlusal surface pictures of P_3, P_4, M_2, C_1, and M_2 to examine the crown outline shapes, the relative position of the anterior and posterior foveae, and the orientation of the occlusal grooves (Fig. 3). Due to the heavy occlusal and interproximal wear of Sh.y.072 (M_2), the GM analysis was carried out on only the dentine surface of the crown reconstructed from the micro-CT scan. Though the occlusal wear on one of the P_4s (Sh.y.007) is heavy, the crown basal area and anterior/posterior foveae, on which the GM analysis is based, were not affected.

 [Insert Figure 3]

Landmarks on the P_3s and P_4s were chosen following the protocol of Gómez-Robles et al. (2011), namely the tips of buccal and lingual cusps, anterior and posterior foveae. However, since the apices of both buccal and lingual cusps of the Yiyuan P_3s and P_4s have been flattened by wear, only the anterior and posterior foveae (Type 1 in Bookstein. [1991]) were used. The crown outlines of P_3 and P_4 were divided into forty equidistant parts by the TpsDig2 program (Rohlf, 1998a), and the dividing points were treated as semi-landmarks (Fig. 3). Equidistantly spaced semi-landmarks do not necessarily guarantee geometric or biological correspondence across specimens. Therefore, the spacing of curve semi-landmarks is arbitrary (Gunz and Mitteroecker, 2013). However, the effect of the arbitrary spacing can be removed by the sliding technique through "optimizing" the positions of the semi-landmarks related to the average shape of the entire sample (Gunz and Mitteroecker, 2013). On the M_2s, three landmarks (Type 1 in Bookstein. [1991]) were chosen: the two points where the extensions of the buccal and mesial occlusal grooves intersect with the crown outline and the central fovea, respectively. The outlines of the protocone, metacone, and hypocone were equidistantly divided with the TpsDig2 program (Rohlf, 1998a) into twenty-one parts, and the paracone outline into nine parts. Four points equidistantly divided the buccal and mesial occlusal grooves into five equal parts. The division follows the principle that each part of the crown outline or occlusal grooves had a roughly equal length, and the dividing points were treated as semi-landmarks (Fig. 3). Wood et al. (1983) showed that the variation in the main fissure pattern in the M_1s and M_2s of a large hominin sample was useful for taxonomic inferences. In Wood et al. (1983), the landmarks are located at the intersections of groove-groove and groove-crown outline. To quantify the groove orientation more precisely, semi-landmarks dividing equally the main occlusal grooves are also used in the present study (Fig. 3). The reason for not using lingual occlusal groove in our analysis is due to the variable occurrence of hypocones in all M_2s.

On the C_1s, no landmark could be defined on the occlusal surfaces. Instead, forty equidistant semi-landmarks were chosen along the outline of the crown using the TpsDig2 program (Rohlf, 1998a).

After the reconstruction of the dentine surface of the M_2s, each 3D model was adjusted with the plane formed by its cemento-enamel junction maximally parallel to the computer monitor. Then a picture of the occlusal view was captured and stored as a JPEG file. At the dentine surface of the M_2s, two landmarks (Type 1 in Bookstein. [1991]) were chosen: the two intersection points between the crown outline and the mesiobuccal and lingual grooves. The outlines of the trigonid and talonid were divided equally, using the TpsDig2 program (Rohlf, 1998a), into twenty parts (Fig. 3). The division follows the principle that each part of the crown outline was roughly equal in length. The dividing points were treated as semi-landmarks.

The TpsDig2 program (Rohlf, 1998a) was employed to digitize landmarks and semi-landmarks, and the whole process was completed by the same person (X.S.). The TpsRelw program (Rohlf, 1998b) was used to undertake superimposition on the raw coordinate data and the relative warp analysis (or principal component analysis) of shape variables.

Description of the Yiyuan teeth

Upper right first premolar (Sh.y.003)

This tooth (Figs. 4 and 5) is well preserved and only the apical third of the lingual root is broken. Occlusal wear corresponds to grade 3 (Molnar, 1971). Both mesial and distal interproximal wear facets are large and ellipsoid in shape. In the distal aspect, at the level of the cement-enamel junction, there is a buccolingually elongated interproximal groove as a result of tooth-picking (Sun et al., 2014).

[Insert Figure 4]

[Insert Figure 5]

The crown outline is oval and slightly asymmetrical, with the mesial half more buccolingually elongated than the distal half. There is no sign of a transverse crest. The essential ridge of the buccal cusp is bifurcated. Both mesial and distal accessory ridges are present. Due to occlusal wear, morphological details of the lingual cusp, as well as the presence/absence of accessory tubercles, cannot be assessed. On the buccal surface, a moderately deep mesial vertical groove runs towards the apex of the buccal cusp, while there is no clear distal vertical groove.

At the EDJ, the occlusal surface is strongly crenulated. The essential crest of the buccal cusp is bifurcated, with the mesial ridge being more pronounced than the distal one. The mesial accessory ridge of the buccal cusp is conspicuous, while the distal accessory ridge is composed of two ridges of different sizes. At the EDJ, we also observe the bifurcation of the essential ridge of the lingual cusp and both mesial and distal accessory ridges. No marginal accessory tubercle is present. On the buccal surface, the mesial vertical groove is relatively deep, while there are two faint distal vertical grooves that circumscribe a shallow V-shaped depression. From the lateral aspect, the buccal side is curved and lacks a cingulum. On the mesial side, the cement-enamel junction runs almost horizontally for most of its length and then suddenly ascends in the direction of root apex at a pronounced angle. The root is composed of a buccal and a lingual radical, which bifurcate from the second third of the root. The roots are robust and rounded in section and they do not narrow until the tip.

Upper left first premolar (Sh.y.004)

This tooth (Figs. 4 and 5) is the antimere of Sh.y.003. Its crown is well preserved, while only half of the buccal root and a small portion of the lingual root remain. The occlusal wear corresponds to grade 3 (Molnar, 1971). Both mesial and distal interproximal wear facets are ellipsoid in shape. There are several enamel pits on the mesial aspect of the buccal surface, probably of taphonomic origin. A distal interproximal groove along the cervical line has been interpreted as a result of tooth-picking (Sun et al., 2014).

Similar to its antimere, this tooth has an oval and asymmetrical crown outline with a more elongated mesial half. No transverse crest is developed. The expression of several secondary fissures complicates the occlusal surface. Whether the essential ridge of the buccal cusp is bifurcated is not clear due to occlusal wear. The preservation of faint secondary grooves suggests that the essential crest of the lingual cusp is bifurcated. Both mesial and distal accessory ridges of the lingual cusp are well developed. On the buccal surface of the crown, a mesial vertical groove is well developed, while the distal vertical groove is shallow. A prominent basal eminence is visible at about 4 mm from the cervical line.

At the EDJ, the essential crest of the buccal cusp is bifurcated, and both mesial and distal accessory ridges are present. The lingual essential crest is also bifurcated and both the mesial and the distal accessory ridges of the lingual cusp are well developed. On the buccal surface, the mesial vertical groove is deep and associated with an enamel elevation, whereas the distal groove appears as a shallow V-shaped depression. The preserved part of the root is deeply furrowed by a broad longitudinal groove on its mesial surface. Two independent canals are visible on the cross-section of the broken roots.

Upper left second premolar (Sh.y.007)

This is a nearly complete tooth (Figs. 4 and 5) with a well-preserved crown and root, except for a mesiobuccal-distolingual crack along the whole tooth. Occlusal wear has considerably reduced the crown height and the pattern of dentine exposure corresponds to grade 4 (Molnar, 1971). Both the mesial and the distal interproximal facets are large and elliptical in shape.

From the occlusal aspect, the crown has an oval and slightly asymmetrical outline, with an abbreviated distolingual corner due to the mesial shift of the lingual cusp. No transverse crest is developed. Due to heavy occlusal wear, only the distal accessory ridge of the buccal cusp and the mesial accessory ridge of the lingual cusp can be identified. On the buccal surface of the crown, the basal prominence is faintly developed. The distal vertical groove is moderately deep, while the identification of its mesial counterpart is obscured by the fracture.

At the EDJ, the essential ridge of the buccal cusp is bifurcated. Both mesial and distal accessory ridges are present. Next to the mesial marginal ridge, two marginal accessory tubercles are identified.

On the buccal surface, the mesial vertical groove is moderately developed, while the distal vertical groove is represented by a weak triangular depression.

A broad and deep longitudinal groove runs along the distal surface of the root, whereas the groove in the mesial surface is weaker. The root is composed of two well-differentiated radicals that are joined by a dentine/cementum lamina except for the tip. The root is robust, with the buccal radical being longer than the lingual one. The root does not narrow until the tip.

Upper left second premolar (Sh.y.071)

A complete crown and a small segment of the root are preserved on Sh.y.071 (Figs. 4 and 5). The pattern of dentine exposure corresponds to occlusal wear of grade 3 (Molnar, 1971). Both mesial and distal interproximal wear facets are large and oval-shaped.

From the occlusal view, the crown has an oval and slightly asymmetrical outline, with an abbreviated distolingual corner due to the mesial shift of the lingual cusp. There is no transverse crest. The essential crest of the buccal cusp is bifurcated. There is a distal accessory ridge on the buccal cusp but no mesial accessory ridge. In the mesial marginal ridge there are four accessory tubercles. On the buccal surface face, the mesial vertical groove is moderately developed, while the distal one is weak. At the EDJ, the essential crest of the buccal cusp is composed of three small ridges and distal to it there is a well-developed distal accessory ridge. The essential crest of the lingual cusp is bifurcated and bordered by well-developed mesial and distal accessory ridges. There are five mesial accessory ridges of different sizes. On the buccal surface, the mesial vertical groove is moderately developed, while the distal one is weakly expressed. The cross section of the preserved root is constricted by the expression of both mesial and distal longitudinal developmental grooves.

Upper right second molar (Sh.y.008)

The crown of Sh.y.008 (Figs. 5 and 6) is complete and presents occlusal wear of grade 2 (Molnar, 1971). There are clear mesial and distal interproximal wear facets. Less than half of the lingual radical and a small part of the mesiobuccal radical are preserved. The enamel shows a mottled defect of pathological/taphonomic origin, particularly evident on the buccal and occlusal surfaces.

[Insert Figure 6]

In occlusal view, the crown outline shape is trapezoidal and mesiodistally compressed, with an obviously abbreviated distobuccal corner and slightly reduced distolingual aspect. The buccolingual dimension of the mesial cusps is predominant over the distal ones. The hypocone is medium-sized (grade 3.5 of ASUDAS). At the mesial aspect, three accessory ridges are detected. The crista obliqua is partially notched by the groove but it is continuous. There is no sign of a transverse crest.

At the EDJ, there are two small ridges next to the distal marginal edge that could correspond to a C5 although it cannot be identified at the enamel surface. In the mesial marginal ridge, there are three accessory ridges of varying sizes. The dentine surface is highly crenulated with the development of several secondary grooves and ridges. There is no transverse crest and the crista obliqua is continuous. On the buccal surface of the paracone, a dentine shelf is moderately developed, and it probably corresponds to the projection of the mesial marginal ridge onto the buccal surface. In the mesiolingual corner of the protocone, two faint vertical grooves could be identified as grade 1 of Carabelli's trait (Ortiz et al., 2012). The preserved fragment of the lingual root is inclined lingually and presents a shallow longitudinal groove on its lingual surface.

Lower right canine (Sh.y.005))

The crown of this tooth (Figs. 5 and 6) is well preserved. The apical third of the root was broken off and reconstructed later. There is some superficial loss of cementum along the root surface. The degree of occlusal wear corresponds to grade 4 (Molnar, 1971). A long crack is evident over the distal aspect of the labial surface. There is a small and round interproximal wear facet on the mesial surface, while the distal interproximal wear facet is missing, likely because of occlusal wear.

From the lingual view, both mesial and distal marginal ridges are thickened and strongly elevated

(shovel shape, grade 4 of ASUDAS), with the distal one being slightly more prominent than the mesial. The basal eminence is moderately developed and from it, a moderately elevated central ridge emerges. On the labial surface, the mesial vertical groove is weak but the distal one is remarkably deep. The vertical grooves at the distal margin of both the labial and lingual surfaces almost delimit a cuspule-like distal marginal ridge.

At the EDJ, the lingual central ridge is also moderately elevated. On the labial surface, a pronounced distal vertical groove is detected. Viewed distally, the marginal ridge almost adopts a cuspule-like aspect due to the development of strong distal vertical grooves on both buccal and lingual faces. The root is robust and thick, with an elliptical cross-section.

Second right lower molar (Sh.y.072)

The crown of this tooth (Figs. 5 and 6) is well preserved, but most of the root is missing. Wear has reduced the occlusal surface to a nearly flat plane and the pattern of dentine exposure corresponds to grade 4 (Molnar, 1971). The interproximal facet can be seen on both the mesial and distal aspects. The mesial interproximal facet is more extensive than the distal. There is an evident interproximal groove along the cervical line formed as a result of tooth-picking (Sun et al., 2014).

In occlusal aspect, the crown has a relatively round outline, markedly elongated buccolingually. The buccal contour of the crown is rounded and smooth and the lingual one is relatively straight. Despite the heavy occlusal wear, it is possible to distinguish the five main cusps on the enamel surface. The hypoconulid is well developed (grade 4 of ASUDAS) and completely buccally displaced. The distal groove bifurcates shortly after originating from the central fovea and encloses a cusp 6, which is smaller than the hypoconulid (grade 2 of ASUDAS). The main five cusps are arranged in a "Y" pattern. However, this pattern is not symmetrical, because the hypoconulid stems from the central fovea and contacts the metaconid through a short groove. A longitudinal fissure in the metaconid delimits a pronounced deflecting wrinkle (grade 2 of ASUDAS). On the buccal surface of the protoconid, there is a secondary groove extending mesially from the buccal groove that defines a prominent protostylid (grade 6 of ASUDAS). No middle or distal trigonid crest (MTC or DTC) is expressed (Type D of Martínez de Pinillos et al., 2014).

At the EDJ, a C6 and a deflecting wrinkle can be detected. The EDJ surface is profusely crenulated due to the existence of extra cusps and several interconnected secondary ridges. There is no sign of a middle or distal trigonid crest. Because of the occlusal dental wear we cannot assess the presence/absence of a middle trigonid crest, but the Yiyuan M_2 probably has either a Type 2 or a Type 4 (Martínez de Pinillos et al., 2014). The protostylid is expressed as a prominent shelf running on the whole buccal surface of the protoconid. There is a conspicuous vertical ridge running from the base of the protostylid cleft to the tip of the protoconid. Judging from the preserved portion of the root, we ascertain the existence of at least two roots bifurcating at about 5 mm away from the cervical line in the lingual view. A broad and deep longitudinal furrow is evident on the mesial surface of the mesial radical.

Results and preliminary discussion

Homo *versus* Pongo *features of Yiyuan teeth*

At present, the only Chinese Pleistocene sites where *Pongo* fossils have been discovered are restricted to the Guizhou, Guangxi, Guangdong, and Yunnan districts (see Zhao et al., 2009). The northern limit of this region is the Yanhui Cave (28°15'N) in Tongzi (Guizhou Province) (see Zhao et al., 2009), ~1300 kilometers from the Yiyuan site of Shandong Province. On the basis of this biogeographic pattern, the teeth are not likely to be *Pongo*. There is also evidence of tooth picking, a behavior argued to be unique to the genus *Homo* (Ungar et al., 2001; Hlusko, 2003) as to date tooth-picking habits have been documented exclusively in the genus *Homo*, including in *Homo habilis* (Ungar et al., 2001), *Homo erectus* (Holden, 2000), *Homo heidelbergensis* (Bermúdez de Castro et al., 1997), *Homo neanderthalensis* (e.g., Lozano et al., 2013), and *Homo sapiens* (e.g., Berryman et al., 1979).

Binocular microscopy and Scanning Electron Microscopy (SEM) on the interproximal surfaces of Yiyuan teeth showed that five out of seven Yiyuan teeth (Sh.y.003, 004, 007, 008, and 072) exhibited different degrees of interproximal wear, ranging from multiple fine striae to deep interproximal grooves (Sun et al., 2014). The locations, morphology and dimensions of both the fine striae and grooves are consistent with artificial wear generated by habitual tooth-picking behavior. The presence of tooth-picking marks in the Yiyuan teeth is thus strong cultural evidence in support of their

assignment as human (Sun et al., 2014).

Metric data are also in support of the teeth being best assigned to *Homo*. In general, the diameters of the Yiyuan teeth are smaller than those of *Pongo,* and most of them are out of the range of *Pongo* variation (Fig. 7). In those cases where the Yiyuan measurements overlap with the *Pongo* distribution (MD of M_2, BL of P_3, M_2, and M_2), they consistently fall in the lower limit of the range of variation and also overlap with the dimensions in a wide range of hominins, particularly those from East Asian Early and Middle Pleistocene hominins.

[Insert Figure 7]

The results of the present study show that the mean RDHH of the paracone and the protocone of *Pongo* specimens are 27.9% and 23.9%, respectively (Table 3). Comparatively, recent modern humans are characterized by higher dentine horns, on average, for both the paracone (39.7%) and the protocone (36.6%). Our values are consistent with those obtained by Olejniczak et al. (2008), where mean RDHHs of the protocone and the paracone of *H. sapiens* are 35.3% and 36.2%, respectively, and for *Pongo* 28.2% and 27.1% respectively. For Yiyuan Sh.y.008 we obtained a RDHH of 35.5% for the protocone and 37.4% for the paracone.

Our results indicate that the Yiyuan Sh.y.008 values are closer to *H. sapiens* than to *Pongo*. In particular, the RDHH of the Sh.y. 008 protocone is higher than the upper limit of the range of variation in *Pongo* for this cusp. The Yiyuan M_2 shows relatively higher dentine horns, as is typical of *H. sapiens* and in contrast to the lower horns of *Pongo* (Olejniczak et al, 2008).

[Insert Table 3]

For P_3, and as shown in Figure 8, all *Pongo* specimens are distributed in the negative-value area of RW1, while both fossil hominins and recent modern humans are plotted at the opposite end. This analysis indicates that *Pongo* P_3s have a highly distorted crown outline, with the mesiobuccal corner being strongly bulged, contrasting with the more symmetrical shapes found in hominins. The anterior and posterior foveae in *Pongo* specimens are widely separated from each other and very close to the marginal ridges, in contrast with the more centered foveae in the rest of the specimens analyzed.

For P_4 (Fig. 8), *Pongo* specimens are mainly plotted towards the negative-value pole of the relative warp (RW) 1 axis, whereas fossil hominins and recent modern humans cluster in the positive-value area. Unlike some hominin specimens, the Yiyuan P_4s are distributed outside the range of variation of *Pongo* specimens, falling at the positive-value end of the RW1 axis. Compared to most of the hominin specimens, *Pongo* P_4s present a relatively wider lingual half, and the foveae are well-separated and very close to the marginal ridges.

GM analyses of the M_2 crown outline shape and orientation of the occlusal grooves show that most of the *Pongo* specimens cluster in the upper left quadrant of the graph, although overlap with other fossil hominins and recent modern humans exists (see Figure 8). The Yiyuan M_2 falls at the extreme right of the range of variation of the *Pongo* sample, in the upper right quadrant, where most of the specimens are hominins. This analysis shows that the occlusal outline and groove orientation of the M_2 are not the best discriminators, so other features, such as the RDHH or the expression of tooth-picking grooves, should be employed to distinguish between *Homo* and *Pongo*.

As shown in Figure 8, the Yiyuan C_1 falls in an area that is occupied exclusively by hominin fossils and recent modern humans. *Pongo* specimens are distributed in the positive-value pole of RW1 with a few fossil hominin and recent modern human specimens, but there is barely any overlap between *Pongo* and hominins. This analysis shows that *Pongo* lower canines tend to show a strongly asymmetrical crown outline with a bulged distolingual corner. The maximum diameter is the BL and it is oblique in a mesiobuccal to distolingual direction. In contrast, most recent modern humans are characterized by an oval and more symmetrical crown outline, where the BL and MD diameters are more balanced, although the MD tends to predominate. The Yiyuan specimen falls within the range of variation of recent modern humans, and is separated from *Pongo* by presenting a more symmetrical crown outline.

For M_2, recent modern humans predominantly occupy the left half of the graph (Fig. 8) and, with a few exceptions, they are well separated from *Pongo* specimens. *Homo sapiens* is characterized by mesiodistally short and rounded crown outlines. In contrast, all but one of the *Pongo* specimens are distributed in the right half of the graph. The *Pongo* M_2s tend to have a mesiodistally elongated crown with a pronounced constriction at the point of contact between trigonid and talonid. The Yiyuan tooth displays the same pattern as modern humans, and occupies the upper left corner of the graphic, far from the *Pongo* area of distribution.

[Insert Figure 8]

In humans, lower canine morphology has evolved from primitive states, characterized by an asymmetrical crown outline, cuspule-like marginal ridges, and a highly elevated lingual central ridge (Moggi-Cecchi et al., 2006; Martinón-Torres et al., 2008) to more simple and incisor-like canines. The canine from Yiyuan, together with most specimens of *H. ergaster*, East Asian Early and Middle Pleistocene hominins (e.g., KNM WT-15000, KNM ER-992, Sangiran 7-59, ZKD 70 and 73) present an intermediate state, with almost cuspal-like marginal ridges and/or elevated lingual central ridges, though to a less extent than the earliest hominins such as *Australopithecus* (Weidenreich, 1937; Wood, 1991; Walker and Leakey, 1993; Grine and Franzen, 1994; Xing, 2012). In contrast, the shape of the *Pongo* C_1 is close to a cone, and displays a bulged distolingual corner when viewed occlusally (Fig. 9). The maximum diameter is oblique in a mesiobuccal to a distolingual direction and is remarkably different from canines of the genus *Homo*, even in those that preserve a primitive pattern and where the projection of the distal marginal ridge provides a more asymmetrical contour. Unlike in the Yiyuan teeth, in *Pongo* canines we cannot find a shovel shape because marginal ridges cannot be identified and lingual fossa is occupied by a strongly elevated lingual central ridge with longitudinal grooves.

[Insert Figure 9]

Pongo molars are generally characterized by a highly crenulated occlusal surface at the OES, particularly due to the expression of several secondary grooves that define numerous ridges. The Yiyuan teeth also present complicated and crenulated surfaces as an expression of a primitive feature for the genus *Homo* that has been ascertained in other hominin assemblages such as those from Sangiran, Zhoukoudian, Hexian or Atapuerca-TD6 (Weidenreich, 1937; Grine and Franzen, 1994; Bermúdez de Castro et al., 1999; Kaifu et al., 2005). At the EDJ, the Yiyuan molars also present a very complicated surface with the definition of a net of interconnected secondary grooves and ridges. This dendritic EDJ surface is different from the one evident in *Pongo* teeth (Fig. 10), where the ridges are less pronounced and elevated and significantly thinner or hair-like. As it has been pointed out, for some primary-definitive traits such as C6, C7, trigonid crest pattern, and protostylid expression, there is a consistent match between OES and EDJ in the presence/absence of a feature (Skinner et al., 2008). However, Skinner et al. (2010) stated that the morphology of the EDJ of *Pongo* was less complicated than the OES. Conversely, the EDJ surfaces of Yiyuan molars are more complicated than the OES and display strong crenulations, and multiple essential crests and ridges that are relatively elevated (Fig. 10). Interestingly, the same type of dendritic EDJ surface found on the Yiyuan molars has been identified in the Zhoukoudian and Hexian specimens and could be a peculiarity of some continental Asian Middle Pleistocene fossils (Fig. 10; Xing et al., 2014).

[Insert Figure 10]

Comparisons between the Yiyuan teeth, other samples of fossil hominins and recent modern humans

Upper first premolar (P3) The transverse crest and bifurcated essential crest of P3 tend to decrease in frequency over time (Wood, 1991; Moggi-Cecchi et al., 2006; Martinón-Torres et al., 2008, 2012; Xing et al., 2014). While the transverse crest is rare, the bifurcation of the essential crest is a relatively common feature in East Asian Middle Pleistocene specimens (e.g., Zhoukoudian, Hexian, Chaoxian or Panxian Dadong; Bailey and Liu, 2010; Xing, 2012; Liu et al., 2013; Xing et al., 2014, 2015) as well as the in the Sangiran Early Pleistocene hominins (but see NG9505 in Zanolli, 2013). A furrowed buccal surface is usually present in earlier hominins including *Australopithecus*, African early *Homo*, *H. ergaster*, Sangiran Early Pleistocene, and Chinese mid-Middle Pleistocene hominins (Moggi-Cecchi et al., 2006; Martinón-Torres et al., 2008, 2012; Gómez-Robles et al., 2011; Xing et al., 2014, 2015), but not in the Chinese late Middle Pleistocene sample from Panxian Dadong (Liu et al., 2013) and the early Late Pleistocene hominins from Xujiayao (Xing et al., 2015). Although a continuous transverse crest is absent, the Yiyuan P3s resemble other East Asian Early and mid-Middle Pleistocene hominins in possessing bifurcated essential crests and marked marginal grooves on the buccal surface. The roots of the Yiyuan P3 are widely divergent, and they barely narrow until the tip, resembling East Asian Early and mid-Middle Pleistocene specimens (Kaifu, 2006; Xing et al., 2014) but being unlike Dmanisi (Martinón-Torres et al., 2008).

Geometric morphometric analysis of P3 crown shape (Fig. 11) indicates that RW1 and RW2 account for 29.68% and 17.54% of the total shape variation of the crown outline and the distance between anterior and posterior foveae. Specimens at the negative values of RW1 are characterized by

an asymmetrical crown outline, where the mesiobuccal and mesiolingual corners bulge and anterior and posterior foveae are widely separated. This area is exclusively occupied by *Australopithecus*, early *Homo*, and *H. erectus* sensu lato. The positive-value area of RW1 is occupied by specimens where the crown outline is wider on the buccal side. The distance between anterior and posterior foveae is shortened. This region is mainly occupied by *H. sapiens* specimens. Compared to those in the negative-value extreme of RW2, specimens at the RW2 positive-value area tend to have a crown outline with the contour of the buccal cusp being bulged and wider than the lingual one. The anterior and posterior foveae are also closer.

The Yiyuan P_3s are displayed in the lower left quadrant (Fig. 11). Except for a few specimens of *H. sapiens*, in this area we find the majority of the *Australopithecu*s and early *Homo*, and some *H. ergaster*, East Asian Early and mid-Middle Pleistocene, European Early and Middle Pleistocene specimens. This analysis reveals the primitive character of the Yiyuan specimens and emphasizes the similarities with other Asian Middle Pleistocene samples (except for Panxian Dadong), although the Zhoukoudian, Chaoxian, and one of the Hexian specimens fall in the positive-value end of the RW2 axis.

[Insert Figure 11]

Upper second premolar (P_4) As was observed in the P_3s, the transverse crest and bifurcated essential crest in P_4 s are more frequent in earlier hominins compared to the later *H. sapiens* (Martinón-Torres et al., 2008, 2012; Xing et al., 2014). The Yiyuan P_4s show primitive features such as several marginal accessory tubercles that are relatively frequent in *Homo* specimens before the Middle Pleistocene (Martinón-Torres, 2006; Martinón-Torres et al., 2008). The Yiyuan P_4s also display bifurcated essential crests, which are moderately frequent in East Asian Middle Pleistocene hominins such as Zhoukoudian and Chaoxian (Bailey and Liu, 2010; Xing, 2012; Xing et al., 2014), but not in the early Late Pleistocene hominins from Xujiayao (Xing et al., 2015).

The number of premolar roots in *H. ergaster*, East Asian Early and mid-Middle Pleistocene, and European Early Pleistocene ranges from three to two (White, 1980; Johanson et al., 1982; Ward et al., 1982; Wood, 1991; Walker and Leakey, 1993; Moggi-Cecchi et al., 2006; Kaifu et al., 2011; Martinón-Torres et al., 2012; Xing et al., 2014). The Yiyuan P_4 presents two roots that are joined by a dentine/cementum lamina except for the apical tip, as also occurs in the Early Pleistocene specimens from Atapuerca-TD6 (Bermúdez de Castro et al., 1999). The roots are robust, without narrowing towards the tip, and unlike European Middle Pleistocene specimens and modern humans (Kaifu, 2006; Martinón-Torres et al., 2012; Xing, 2012).

Geometric morphometric analysis of the P_4 (Fig. 12) indicates that RW1 and RW2 account for 23.91% and 22.75% of the total shape variation of the crown outline and the distance between anterior and posterior foveae. Teeth distributed along the positive-value end of RW1 tend to have bucco-lingually elongated crowns, and a relatively large inter-foveae distance. This area is mostly occupied by *Australopithecus* and East Asian Early and Middle Pleistocene specimens, including Yiyuan. In contrast, at the negative end of the RW1 axis, specimens tend to show more balanced BL and MD diameters, a relatively narrower lingual half and a reduced inter-fovea distance. Specimens plotted against the positive-value of RW2 tend to have a crown outline that is bucco-lingually shortened and relatively wide in its lingual half. The anterior and posterior foveae are widely separated from each other. Apart from a few specimens of East Asian Early and mid-Middle Pleistocene and fossil *H. sapiens*, most fossil hominins are distributed in the positive-value area of RW2 whereas the negative-value area is mostly occupied by recent modern humans. In relation to other Early and Middle Pleistocene hominins, the Yiyuan P_4s fall closer to the Sangiran and Zhoukoudian specimens, and have more negative values along the RW2 axis than most of the early *Homo*, *H. ergaster*, and European Middle Pleistocene specimens.

[Insert Figure 12]

Upper second molar (M_2) The hypocone size of the Yiyuan M_2, scored by the ASUDAS (not measured as follows), can be included in the variation of *H. ergaster* and East Asian Early and mid-Middle Pleistocene samples. The early Late Pleistocene hominin from Xujiayao could also fit within this (Xing et al., 2015). The hypocone size in *H. ergaster* and East Asian and mid-Middle Pleistocene hominins is clearly reduced compared to those of *Australopithecus* and African Early *Homo* (Suwa, 2007; Martinón-Torres et al., 2008; Xing et al., 2014), but is still larger than in European Middle Pleistocene specimens, Neanderthals, and modern humans (Martinón-Torres et al., 2012; Xing, 2012).

The M$_2$ relative cusp areas (Fig. 13) indicate that relative paracone size tends to increase in later *Homo* compared to the earliest hominins (*Australopithecus* and early *Homo*), although a certain degree of overlap among taxa exists. The relative paracone area of Yiyuan M$_2$ falls into the range of variation of the earliest hominins, *H. ergaster*, East Asian Early and mid-Middle Pleistocene, European Middle Pleistocene, Neanderthals, and *H. sapiens*. The relative metacone area of Yiyuan M$_2$ is distributed within the range of variation of *Australopithecus*, East Asian Early Pleistocene, Neanderthals, and *H. sapiens*. However, it is out of the range of variation of *H. ergaster* and East Asian mid-Middle Pleistocene specimens. The relative protocone area of the Yiyuan M$_2$ is larger than all specimens of the East Asian Early and Middle Pleistocene, as well as those of the West Asian Early Pleistocene. In the hypocone, there is a trend of decreasing relative size from earliest hominins to later *Homo* species. The size of the Yiyuan M$_2$ hypocone falls into the range of variation of *H. ergaster*, East Asian mid-Middle Pleistocene, European Middle Pleistocene, and *H. sapiens*. It is larger than the hypocones of East Asian and West Asian Early Pleistocene specimens.

The relative size sequence of the M$_2$ cusps also exhibits intergroup variations. In *Australopithecus*, the protocone is the largest cusp of all, and the relative size of the other three vary among specimens. The relative protocone area is largest in early *Homo*. The paracone is smaller than protocone, but larger than both the metacone and hypocone. The relative size sequence of *H. ergaster* and Sangiran Early Pleistocene is either protocone>paracone>metacone>hypocone, or protocone>paracone>hypocone>metacone. Together with the samples of East Asian mid-Middle Pleistocene, Neanderthal lineage, and other later *H. sapiens*, the Yiyuan M$_2$ sequence of relative cuspal size is protocone>paracone>metacone>hypocone.

[Insert Figure 13]

The GM analysis of the M$_2$ (Fig. 14) shows that the first two relative warps account for 40.51% and 19.50% of the total variation of the crown outline shape and the orientation of occlusal grooves, respectively. The specimens at the positive-value half of RW1 present a wider buccal contour and a bulging larger paracone in comparison to the specimens at the negative-value, where the lingual contour is wider because of an expanded hypocone and a reduced paracone. In the positive area of RW1, the buccal and mesial grooves are oblique in relation to the buccolingual and mesiodistal axis of the crown, respectively, and form an obtuse angle between them, whereas in the negative pole the angle between the buccal and the mesial grooves is almost 90°. At the positive-value area of RW2, specimens are characterized by a trapezoidal crown outline with a symmetrically reduced distal half. Both buccal and lingual contours converge distally. Specimens at the negative-value of RW2 show a strongly oblique buccal contour due to a reduced metacone and a bulging paracone. The angle between the buccal and mesial grooves is obtuse in these specimens.

As seen in Figure 14, earliest hominins (i.e., *Australopithecus* and early *Homo*) can generally be separated from recent modern humans along the RW1 axis, with the former being distributed in the left half. Early modern humans, European Early and Middle Pleistocene hominins, and Neanderthals are scattered on the four quadrants, but they tend to present positive values on RW1. The Yiyuan tooth is located in the upper right quadrant (Fig. 14), together with most of the mid-Middle Pleistocene hominins from East Asia, except for Chaoxian, and is separated from most of the *H. ergaster* and East Asian Early Pleistocene samples.

[Insert Figure 14]

The EDJ surface of Yiyuan M$_2$ is as crenulated as the EDJ surfaces reported for the Hexian hominins (Fig. 10). The surface is characterized by the expression of several mesial marginal tubercles, secondary furrows, and bifurcated essential crests that conform to a dendritic pattern similar to that found in Zhoukoudian and Hexian specimens.

Lower canine (C$_1$) As stated above, the canine from Yiyuan, together with other *H. ergaster*, East Asian Early and Middle Pleistocene specimens (e.g., KNM WT-15000, KNM ER-992, Sangiran 7-59, ZKD 70 and 73) and *H. antecessor* (Bermúdez de Castro et al., 1999) present an intermediate state, with nearly cuspal-like marginal ridges and an elevated lingual central ridge, though to a lesser extent than *Australopithecus,* African early *Homo* and the Dmanisi specimens (Weidenreich, 1937; Wood, 1991; Walker and Leakey, 1993; Grine and Franzen, 1994; Xing, 2012). The Yiyuan canine is also different to that found in other samples such as in specimens from the East Asian late Middle Pleistocene site of Panxian Dadong, European Middle Pleistocene populations, Neanderthals, and modern humans, where more simple and incisor-like patterns can be identified (Martinón-Torres et al., 2012; Xing, 2012; Liu et al., 2013).

Lower second molar (M_2) The combination of a well-developed hypoconulid in a clear buccal position, C6, and deflecting defecting wrinkle, as occurs in the Yiyuan specimen, is more frequent in *Australopithecus*, African Early *Homo*, *H. ergaster*, East Asian Early and mid-Middle Pleistocene samples than in the European Middle Pleistocene hominins, Neanderthals, and modern human assemblages (Martinón-Torres et al., 2012; Xing et al., 2014, but see the Bapang M_2s reported in Zanolli, 2013). Although the groove pattern of Sh.y.072 is a "Y" type, the pattern is asymmetrical due to the contact between the hypoconulid and the metaconid. This type of arrangement is rare and could be detected in the Dmanisi sample (Martinón-Torres et al., 2008) and some East Asian Early and mid-Middle Pleistocene specimens from Sangiran and Zhoukoudian (Sangiran 5 and 7-78, ZKD 107) (Grine and Franzen, 1994, Xing, 2012).

The protostylid of Sh.y.072 is cleft-like and occupies almost the whole buccal surface of the protoconid. Besides those found in *Australopithecus* and African Early *Homo* (Hlusko, 2004), this conspicuous, long, and band-like protostylid is generally found in Early Pleistocene samples such as those from Dmanisi (Martinón-Torres et al., 2008) and Sangiran 6, and some mid-Middle Pleistocene specimens from Zhoukoudian (Weidenreich, 1937). However, the most remarkable feature of the Yiyuan protostylid is found at the EDJ. The EDJ surface of Yiyuan M_2 is as crenulated as those reported in Zhoukoudian and Hexian hominins (Fig. 10), and more complicated than those from the European Middle Pleistocene, Neanderthals, and *H. sapiens* (Bailey et al., 2011; Martínez de Pinillos et al., 2014; Martinón-Torres et al., 2014; Xing et al., 2014), and Sangiran (as reported by Zanolli [2015]). Although available data on the EDJ surface from hominins are limited, it seems that the Yiyuan EDJ is also more crenulated than in some *Australopithecus* specimens (Skinner et al., 2008) and the Tighenif specimens (Zanolli et al., 2010). The crenulated dental surface common in the Yiyuan, Hexian, and Zhoukoudian M_2s involves the expression of a C6 or/and C7, the bifurcation of the essential crests, and the expression of accessory ridges. In the case of the Sangiran M_2s (NG0802.3 and NG92 D6 ZE 57s/d 76; Zanolli, 2015), both teeth have only four main cusps, and along with the hypoconulid, the C6 and the C7 are also absent. In addition, the essential crest and accessory ridges of the main cusps in this Sangiran subsample are much less developed than those in Yiyuan, Hexian, and Zhoukoudian. On the buccal surface, the pronounced to moderately-expressed protostylid in Yiyuan, Hexian, and Zhoukoudian contrasts with its weak expression in the Sangiran M_2s studied by Zanolli (2015). Particularly, there is a vertical and conspicuous crest running from the base of the protostylid shelf to the protoconid that has been noted only in Hexian (Xing et al., 2014) and Zhoukoudian molars (Xing et al., 2015), and in a less pronounced form in a few Middle Pleistocene specimens from Atapuerca SH (AT-100, AT-1473, AT-2271; Martínez de Pinillos et al., 2014). This feature is not reported in either Indonesian *H. erectus* molars (Zanolli, 2015) or in the East African late Early Pleistocene *H. erectus/ergaster* specimen MA 93 (Zanolli et al., 2014). The evolutionary significance of this feature requires further study in larger samples.

It is noteworthy that a continuous mid-trigonid crest as is typically documented in European Middle Pleistocene hominins and Neanderthals (Bailey et al., 2011; Martínez de Pinillos et al., 2014) is not found in the Yiyuan, Hexian, and Zhoukoudian samples. The Type D of MTC at the enamel and Types 2 or 4 at the EDJ are among the least frequent types for the Neanderthal lineage (Bailey et al., 2011; Martínez de Pinillos et al., 2014, 2015).

Metric comparison Except for the canine, the size of the other four dental elements from Yiyuan is outside the range of variation of the European Early and Middle Pleistocene specimens, Neanderthals, and early and recent modern humans (SI Fig. 1). Compared to Zhoukoudian, the Yiyuan hominins have a relatively larger M_2, and smaller C_1 and M_2 (mainly in the MD dimension). The smallest of the Yiyuan M_2s is also outside the range of the East Asian Early Pleistocene sample. The main differences between the Yiyuan specimens and *H. ergaster* are larger Yiyuan M_2 BL dimension, and smaller MD dimension for the C_1 and the M_2. For P_3, P_4, and M_2, the Yiyuan teeth have a similar crown size to those from Chaoxian. The Panxian Dadong hominins, despite belonging to the East Asian Late Middle Pleistocene, present smaller P_3s and C_1s than do Yiyuan specimens.

Discussion and conclusion

Based on the varied array of analyses performed (as summarized in Table 4), the Yiyuan hominins can be differentiated from those of fossil *Pongo* from Pleistocene China. The crown sizes of Yiyuan teeth are generally smaller than those of *Pongo*, except for the M_2, although for this dental class the overlap affects almost all the studied hominin groups. In addition, evidence of tooth-picking, which has been found exclusively in *Homo*, is found on five out of seven teeth and in all the individuals. The relative dentine horn height in the Yiyuan M_2 is particularly discriminatory and characteristic of humans

(Olejniczak et al, 2008). Geometric morphometric analyses on the crown outline of OES/EDJ, the relative position of the foveae, and groove orientation also differentiate the Yiyuan teeth from those of fossil *Pongo*, except for the M_2, where there is an overlap among *Pongo* and fossil hominins. However, although GM analysis of M_2 shape does not differentiate *Pongo* and human species, the RDHH and the expression of a tooth-pick groove in the Yiyuan M_2 remain strong evidence in favor of the Yiyuan teeth being human.

We acknowledge that the particular EDJ morphology of the Yiyuan teeth is not commonly seen in other Pleistocene hominins and modern humans. However, we have shown that the dendritic pattern shown by the Yiyuan hominins is different from that of *Pongo* and very similar to that displayed by other Middle Pleistocene hominins from continental Asia, such as Zhoukoudian and Hexian, and could be a peculiarity of the hominin populations from this period and region (see below). In sum, the Yiyuan dental sample can be distinguished from fossil *Pongo* teeth based on geographic, behavioral, morphological (internal and external) and morphometric features.

[Insert Table 4]

In comparison with other hominin groups, and in particular with the East Asian Early and Middle Pleistocene hominins, the Yiyuan teeth display several primitive traits relative to the *Homo* clade, which mainly involve complexity of the occlusal surface, crown buttressing features, robust root structure, crown outline shape, and large crown size. More precisely, the occlusal surfaces are complicated due to the expression of C6, deflecting wrinkles, and the development of several secondary grooves that define the expression of bifurcated essential crests in upper premolars. The buttressing system refers to features that add morphological robusticity, also called mass-additive traits by Irish (1998). We include in these the elevation of the lingual central ridge, the cuspule-like distal marginal ridge of the C_1, the buccal vertical grooves of the P_3s as a type of cingulum-derived feature, and the protostylid of the M_2. The root structure of the Yiyuan P_3 is represented by two independent, robust and highly divergent radicals. The asymmetrical crown outlines of Yiyuan P_3s and P_4s are also primitive owing to a conspicuous talon.

The primitive morphological pattern exhibited by the Yiyuan specimens distinguishes them from the European Middle Pleistocene hominins, Neanderthals, and modern humans. The European Early Pleistocene teeth (*H. antecessor*) are similar to those of the Yiyuan specimens in the expression of some primitive traits, such as the extensive development of secondary grooves on the occlusal surface of posterior teeth and the two-rooted premolars (Bermúdez de Castro et al., 1999). However, some of the buttressing features, such as the vertical grooves on the buccal surface of P_3, are more pronounced in the Yiyuan specimens. Features that have been classically considered as typical of the Neanderthal lineage (Bailey, 2002, 2004; Martinón-Torres et al., 2006; Gómez-Robles et al., 2007, 2008; Bailey et al., 2011), such as the high and continuous mid-trigonid crest of lower molars, are not observed in the Yiyuan M_2. In addition, the Yiyuan teeth are different from those of *H. ergaster* (or African *H. erectus*) in shape and size. Comparatively, the Yiyuan P_4, M_2, and M_2 are bucco-lingually elongated. The measurement of the relative cuspal area also shows that the Yiyuan M_2 has a relatively smaller protocone than *H. ergaster*.

The Yiyuan teeth retain similar primitive morphologies to other East Asian mid-Middle Pleistocene hominins. In addition, the skull recovered with the Yiyuan teeth exhibits features that are considered typical of East Asian *H. erectus*, namely the marked frontal recession, postorbital constriction, deep postorbital sulcus, and strong supraorbital torus (Lu et al., 1989; Wu and Poirier, 1995). However, a series of dental studies on East Asian Middle Pleistocene hominins (i.e., Zhoukoudian, Chaoxian, Hexian, Panxian Dadong) recently revealed that the morphological diversity of East Asian Middle Pleistocene hominins is greater than previously thought (Zhang and Liu, 2002; Bailey and Liu, 2010; Xing, 2012; Liu et al., 2013; Xing et al., 2014). Except for the smaller canine dimensions, the morphology of the C_1 and the P_4 (Sh.y.005 and 007) from Yiyuan Locality 1 are similar to those from Zhoukoudian and Chaoxian although different from the more derived canine from Panxian Dadong (Liu et al., 2013; this study). The occlusal outlines of the P_4s recovered at both Yiyuan and Chaoxian are more buccolingually elongated compared to those of *H. ergaster*. Except for having a relatively larger M_2 and a relatively smaller M_2, the Yiyuan teeth from this locality are similar to those of Zhoukoudian as shown by the GM analysis. Compared to the Hexian sample, the morphology of the P_3 and the M_2, as well as the crown outline shape of the P_3, the M_2, and the M_2 are quite similar, although the Yiyuan P_3 is not three-rooted as in Hexian (Xing et al., 2014). Also, the long, shelf-like protostylid of the Yiyuan M_2 is not observed in the Hexian sample but its morphology at the EDJ presents some interesting resemblances. The relative protocone and metacone areas of the

Yiyuan M2 cannot be included in the range of variation represented by the Zhoukoudian and Hexian teeth. The Yiyuan and Chaoxian hominins resemble each other in the external morphology of the P3, the P4, and the M2, as well as in the crown outline shapes of the P3 and the P4, but they are different regarding the crown outline shape of the M2. In contrast, the P3 of Panxian Dadong has been described as having some modern human-like features (Liu et al., 2013), and its symmetrical crown outline and simplified occlusal surface are clearly more derived than those of the Yiyuan teeth. Some of these derived features can be also found in the Late Pleistocene fossils from Xujiayao, but the Xujiayao P4 and M2 are notably more primitive and closer to the Yiyuan specimens (Xing et al., 2015).

Based on dental morphology, the East Asian Middle Pleistocene hominins (Yiyuan, Zhoukoudian, Chaoxian, Hexian, and Panxian Dadong) could be classified into two types. The first type includes specimens that are usually interpreted as representative of classic *H. erectus* such as those from Zhoukoudian Locality 1 and Hexian. In this context, Hexian would share more primitive features with the chronologically older Sangiran specimens (but see Zanolli, 2013) than either Yiyuan or Zhoukoudian. The Chaoxian teeth from late Middle Pleistocene could also group with the Zhoukoudian *H. erectus*. However, other skeletal parts recovered at Chaoxian (i.e., maxilla and occipital; see Xu et al., 1984) have been interpreted as less typical of Asian *H. erectus* in presenting a weak occipital torus, a depression similar to the fossa supratoralis, a large occipital curvature angle and thinner bone. These differences were the reason that some researchers identified the Chaoxian material as archaic *H. sapiens* (Xu et al., 1984). Although our study does not follow the same terminology and interpretive framework as that employed by Zhang and Liu (2002) and Sun et al. (2011), we acknowledge that the term "archaic *H. sapiens*" can refer to "intermediate" forms that are morphologically more advanced than *H. erectus*, but still more primitive than modern humans. However, and despite some differences in the preservation/loss of primitive features, the Yiyuan skull has been described as being similar to Zhoukoudian *H. erectus*, in the marked frontal recession, postorbital constriction, deep postorbital sulcus, and strong supraorbital torus (Lu et al., 1989, Wu and Poirier, 1995).Thus, from a dental perspective, and with the preservation of more primitive features in the case of Hexian, we find that Zhoukoudian, Chaoxian, and Hexian samples form a morphologically coherent group.

The second type of dental morphology in the Chinese Middle Pleistocene is currently represented by the Panxian Dadong fossils (Liu et al., 2013; Martinón-Torres et al., 2016). Liu et al. (2013) found that some features of the Panxian Dadong teeth fall into the range of variation of modern humans, including the symmetrical crown outline shape and the simplified occlusal surface of upper and lower premolars, the incisor-like lower canine, and the reduced talonid of the P3. Compared to these two groups, our study shows that the Yiyuan hominins are closer to the Zhoukoudian*,* Hexian, and Chaoxian hominins than to the Panxian Dadong sample. The differences between these samples and Panxian Dadong may be related to a complex evolutionary scenario in continental Asia with fragmentation and/or regional variation by isolation (see Dennell, 2009; Zanolli, 2013, 2015; Xing et al., 2014; Martinón-Torres et al., 2016). It would also be in line with the differences found between Northern and Southern China during the Late Pleistocene (Liu et al., 2015).

In our opinion, Zhoukoudian, Yiyuan, Chaoxian and Hexian show a general dental bauplan that could be typical of Asian Early and Middle Pleistocene samples and that includes relatively bucco-lingually elongated mesial cusps compared to the distal ones in the upper and lower molars, as well as the stout, round in section and non-narrowing roots (Kaifu et al., 2005; Xing et al., 2014, 2015; Martinón-Torres et al., 2016). However, Yiyuan, Zhoukoudian and Hexian also present some features that may be unique to these groups, such as the development of a network of interconnected secondary grooves and ridges at the EDJ, especially in the molars. This complex dendritic EDJ surface has not been documented in the currently available EDJ images of other hominins such as *Australopithecus*, North Africa Middle Pleistocene hominins, European Early and Middle Pleistocene hominins, Sangiran *H. erectus* (Zanolli, 2015), Panxian Dadong (Liu et al, 2013), Neanderthals, and *H. sapiens* (Skinner et al., 2008; 2010; Bailey et al., 2011; Martínez de Pinillos et al., 2014, 2015; Martinón-Torres et al., 2014; Zanolli, 2015). In addition, the Yiyuan lower molar also presents a clear vertical ridge running from the protoconid to the protostylid-cleft at the buccal surface. This feature has so far been identified only in Hexian (Xing et al., 2014), Zhoukoudian and some isolated specimens from Atapuerca-SH (see Martínez de Pinillos et al., 2014), and could represent either another shared feature of continental Eurasian Middle Pleistocene humans (see also Martinón-Torres et al., 2007) or one acquired independently in European and continental Asian demes. The EDJ

morphologies of some Sangiran specimens were different from those of Yiyuan, Zhoukoudian, andHexian, as they are not highly crenulated, they lack any protostylid expression and buccal vertical ridge, and show higher dentine horns (Zanolli, 2015).

Future and systematic studies with micro-CT and/or more dental findings will contribute to a better understanding of the evolutionary meaning of the EDJ pattern of Yiyuan, Zhoukoudian, and Hexian hominins. If confirmed to be exceptional, this uniqueness will be relevant for reconstruction of the evolutionary history of genus *Homo* in Asia. The severe climatic oscillations and the vast desert areas that dominated Asia during the Middle Pleistocene (Dennell, 2009; Dennell, 2013; Zanolli, 2013, 2015; Martinón-Torres et al., 2016) have likely favored a pattern of isolation and regional variation. Thus, the possibility that mid-latitude continental Asian groups had a different evolutionary trajectory compared to the penecontemporaneous southeastern Asian *H. erectus* sensu stricto (s.s.) groups should be considered. Our study supports the notion that the taxonomy of the Pleistocene hominins from Asia may have been oversimplified. Futures studies should explore the variability of the Asian specimens and reconsider whether all these samples can be assigned to *H. erectus* s.s.

Acknowledgments

References

Adams, D.C., Rohlf, F.J., Slice, D.E., 2004. Geometric morphometrics: ten years of progress following the 'revolution'. Ital. J. Zool. 71, 5-16.

Arambourg, C., Biberson, P., 1956. The fossil human remains from the Paleolithic site of Sidi Abderrahman (Morocco). Am. J. Phys. Anthropol. 14, 467-489.

Arif, J., Kaifu, Y., Baba, H., Suparka, M.E., Zaim, Y., Setoguchi, T., 2002. Preliminary observation of a new cranium of *Homo erectus* (Tjg-1993.05) from Sangiran, Central Jawa. Anthropol. Sci. 110, 165-177.

Bailey, S.E., 2002. A closer look at Neanderthal postcanine dental morphology: The mandibular dentition. Anat. Rec. 269, 148-156.

Bailey, S.E., 2004. A morphometric analysis of maxillary molar crowns of Middle-Late Pleistocene hominins. J. Hum. Evol. 47, 183-198.

Bailey, S.E., Liu, W., 2010. A comparative dental metrical and morphological analysis of a Middle Pleistocene hominin maxilla from Chaoxian (Chaohu), China. Quatern. Int. 211, 14-23.

Bailey, S.E., Skinner, M.M., Hublin, J.-J., 2011. What lies beneath? An evaluation of lower molar trigonid crest patterns based on both dentine and enamel expression. Am. J. Phys. Anthropol. 145, 505-518.

Bermúdez de Castro, J., 1988. Dental remains from Atapuerca/Ibeas (Spain) II. Morphology. J. Hum. Evol. 17, 279-304.

erm dez de Castro, J.M., rsuaga, J. ., Carbonell, E., Rosas, ., Mart nez, I., Mosquera, M., 1997. A hominid from the Lower Pleistocene of Atapuerca, Spain: Possible ancestor to Neandertals and

modern humans. Science 276, 1392-1395.

Bermúdez de Castro, J.M., Rosas, A., Nicolás, M.E., 1999. Dental remains from Atapuerca-TD6 (Gran Dolina site, Burgos, Spain). J. Hum. Evol. 37, 523-566.

Berryman, H.E., 1979. Non-carious interproximal grooves in Arikara Indian dentitions. Am. J. Phys. Anthrop. 50, 209-212.

Bookstein, F.L., 1991. Morphometric Tools for Landmark Data. Cambridge University Press, Cambridge.

Bookstein, F.L., 1997. Landmark methods for forms without landmarks: morphometrics of group differences in outline shape. Med. Image Anal. 1, 225-243.

Bookstein, F.L., 1999. Linear methods for nonlinear maps: Procrustes fits, thin plate splines, and the biometric analysis of shape variability. In: Toga, A.W. (Eds.), Brain Warping. Academic Press, San Diego, pp. 157–181.

Carbonell, E., Bermúdez de Castro, J.M., Arsuaga, J.L., Allue, E., Bastir, M., Benito, A., Cáceres, I.,

29

Canals, T., Díez, J.C., van der Made, J., Mosquera, M., Ollé, A., Pérez-González, A., Rodríguez, J., Rodríguez, X.P., Rosas, A., Rosell, J., Sala, R., Vallverdú, J., Vergés, J.M., 2005. An Early Pleistocene hominin mandible from Atapuerca-TD6, Spain. Proc. Natl. Acad. Sci. 102, 5674-5678.

Ciochon, R.L., 2010. Divorcing hominins from the Stegodon-Ailuropoda fauna: new views on the antiquity of hominins in Asia. In: Fleagle, J.G., Shea, J.J., Grine, F.E., Baden, A.L., Leakey, R.E. (Eds.), Out of Africa I: The First Hominin Colonization of Eurasia. Vertebrate Paleobiology and Paleoanthropology, Springer, Dordrecht, pp. 111-126.

Dennell, R., 2009. The palaeolithic settlement of Asia. Cambridge University Press, Cambridge.

Dennell, R.W., 2013. Hominins, deserts, and the colonisation and settlement of continental Asia. Quatern. Int. 300, 13-21.

Gómez-Robles, A., Martinón-Torres, M., Bermúdez de Castro, J.M., Margvelashvili, A., Bastir, M., Arsuaga, J.L., Pérez-Pérez, A., Estebaranz, F., Martínez, L.M., 2007. A geometric morphometric analysis of hominin upper first molar shape. J. Hum. Evol. 53, 272-285.

Gómez-Robles, A., Martinón-Torres, M., Bermúdez de Castro, J.M., Prado, L., Sarmiento, S., Arsuaga, J.L., 2008. Geometric morphometric analysis of the crown morphology of the lower first premolar of hominins, with special attention to Pleistocene *Homo*. J. Hum. Evol. 55, 627-638.

Gómez-Robles, A., Martinón-Torres, M., Bermúdez de Castro, J.M., Prado-Simón, L., Arsuaga, J.L., 2011. A geometric morphometric analysis of hominin upper premolars. Shape variation and morphological integration. J. Hum. Evol. 61, 688-702.

Gabunia, L., Vekua, A., Lordkipanidze, D., Swisher, C.C.3rd, Ferring, R., Justus, A., Nioradze, M., Tvalchrelidze, M., Antón, S.C., Bosinski, G., Jöris, O., Lumley, M.-A., Majsuradze, G., Mouskhelishvili, A., 2000. Earliest Pleistocene hominid cranial remains from Dmanisi, Republic of Georgia: Taxonomy, geological setting, and age. Science 288, 1019-1025.

Grine, F.E., Franzen, J.L., 1994. Fossil hominid teeth from the Sangiran Dome (Java, Indonesia). Cour. ForschInst. Senckenberg171, 75-103.

Gunz, P., Mitteroecker, P., 2013. Semilandmarks: a method for quantifying curves and surfaces. Hystrix-the Italian Journal of Mammalogy 24, 103-109..

Han, F., Sun, C., Bahain, J.-J., Zhao, J., Lin, M., Xing, S., Yin, G., 2015. Coupled ESR and U-series dating of fossil teeth from Yiyuan hominin site, northern China. Quatern. Int. doi:10.1016/j.quaint.2015.05.052

Hlusko, L J., 2003. The oldest hominid habit? Experimental evidence for toothpicking with grass stalks. Curr. Anthropol. 44, 738-741.

Hlusko, L.J., 2004. Protostylid variation in *Australopithecus*. J. Hum. Evol. 46, 579-594.

Holden, C., 2000. Man, the toothpick user. Science 288, 607.

30

Irish, J.D., 1998. Ancestral dental traits in recent Sub-Saharan Africans and the origins of modern humans. J. Hum. Evol. 34, 81-98.

Jacob, T., 1973. Palaeoanthropological discoveries in Indonesia with special reference to the finds of the last two decades. J. Hum. Evol. 2, 473-485.

Jin, C., Qin, D., Pan, W., Tang, Z., Liu, J., Wang, Y., Deng, C., Zhang, Y., Dong, W., Tong, H., 2009. A newly discovered *Gigantopithecus* fauna from Sanhe Cave, Chongzuo, Guangxi, South China. Chin. Sci. Bull. 54, 788-797.

Johanson, D.C., White, T.D., Coppens, Y., 1982. Dental remains from the Hadar formation, Ethiopia: 1974–1977 collections. Am. J. Phys. Anthropol. 57, 545-603.

Kaifu, Y., 2006. Advanced dental reduction in Javanese *Homo erectus*. Anthropol. Sci. 114, 35-43.

Kaifu, Y., Aziz, F., Baba, H., 2005. Hominid mandibular remains from Sangiran: 1952–1986 collections. Am. J. Phys. Anthropol. 128, 497-519.

Kaifu, Y., Zaim, Y., Baba, H., Kurniawan, I., Kubo, D., Rizal, Y., Arif, J., Aziz, F., 2011. New reconstruction and morphological description of a *Homo erectus* cranium: Skull IX (Tjg-1993.05) from Sangiran, Central Java. J. Hum. Evol. 61, 270-294.

Liu, W., Schepartz, L.A., Xing, S., Miller-Antonio, S., Wu, X.J., Trinkaus, E., Martinón-Torres, M., 2013. Late Middle Pleistocene hominin teeth from Panxian Dadong, South China. J. Hum. Evol. 64, 337-355.

Liu, W., Martinón-Torres, M., Cai, Y., Xing, S., Tong, H., Pei, S., Jan Sier, M., Wu, X., Edwards, R.L., Cheng, H., Li, Y., Yang, X., Bermúdez de Castro J.M., Wu, X., 2015. The earliest unequivocally modern humans in southern China. Nature 526, 696-699.

Lozano, M., Subirà, M.E., Aparicio, J., Lorenzo, C., Gómez-Merino, G., 2013. Toothpicking and periodontal disease in a Neanderthal specimen from Cova Foradà site (Valencia, Spain). PLoS ONE 8, e76852.

Lu, Z., Huang, W., Li, P., Meng, Z., 1989. Yiyuan fossil man. Acta Anthropol. Sinica 8, 301-313.

Martínez de Pinillos, M., Martinón-Torres, M., Skinner, M.M., Arsuaga, J.L., Gracia-Téllez, A., Martínez, I., Martín-Francés, L., Bermúdez de Castro, J.M., 2014. Trigonid crests expression in Atapuerca-Sima de los Huesos lower molars: Internal and external morphological expression and evolutionary inferences. C. R. Palevol 13, 205-221.

Martínez de Pinillos, M., Martinón-Torres, M., Martín-Francés, L., Arsuaga, J.L., Bermúdez de Castro, J.M., 2015. Comparative analysis of the trigonid crests patterns in *Homo antecessor* molars at the enamel and dentine surfaces. Quatern. Int. http://dx.doi.org/10.1016/j.quaint.2015.08.050.

Martinón-Torres, M., 2006. Evolución del aparato dental en homínidos: estudio de los dientes humanos del Pleistoceno de la Sierra de Atapuerca (Burgos). Ph.D. Dissertation, Universidad de Santiago de Compostela.

31

Martinón-Torres, M., Bastir, M., Bermúdez de Castro, J.M., Gómez, A., Sarmiento, S., Muela, A., Arsuaga, J.L., 2006. Hominin lower second premolar morphology: evolutionary inferences through geometric morphometric analysis. J. Hum. Evol. 50, 523-533.

Martinón-Torres, M., Bermúdez de Castro, J.M., Gómez-Robles, A., Arsuaga, J.L., Carbonell, E., Lordkipanidze, D., Manzi, G., Margvelashvili, A., 2007. Dental evidence on the hominin dispersals during the Pleistocene. Proc. Natl. Acad. Sci. 104, 13279-13282.

Martinón-Torres, M., Bermúdez de Castro, J.M., Gómez-Robles, A., Margvelashvili, A., Prado, L., Lordkipanidze, D., Vekua, A., 2008. Dental remains from Dmanisi (Republic of Georgia): Morphological analysis and comparative study. J. Hum. Evol. 55, 249-273.

Martinón-Torres, M., Bermúdez de Castro, J.M., Gómez-Robles, A., Prado-Simón, L., Arsuaga, J.L., 2012. Morphological description and comparison of the dental remains from Atapuerca-Sima de los Huesos site (Spain). J. Hum. Evol. 62, 7-58.

Martinón-Torres, M., Martínez de Pinillos, M., Skinner, M.M., Martín-Francés, L., Gracia-Téllez, A., Martínez, I., Arsuaga, J.L., Bermúdez de Castro, J.M., 2014. Talonid crests expression at the enamel–dentine junction of hominin lower permanent and deciduous molars. C. R. Palevol 13, 223-234.

Martinón-Torres, M., Song, X., iu, W., erm dez de Castro, J.M., 2016. "source and sink" model for East Asia? Preliminary approach through the dental evidence. C. R. Palevol. doi:10.1016/j.crpv.2015.09.011

Moggi-Cecchi, J., Grine, F.E., Tobias, P.V., 2006. Early hominid dental remains from Members 4 and 5 of the Sterkfontein Formation (1966–1996 excavations): Catalogue, individual associations, morphological descriptions and initial metrical analysis. J. Hum. Evol. 50, 239-328.

Molnar, S., 1971. Human tooth wear, tooth function and cultural variability. Am. J. Phys. Anthropol. 34, 175-189.

Olejniczak, A.J., 2006. Micro-computed tomography of primate molars. Ph.D. Dissertation, Stony Brook University.

Olejniczak, A.J., Smith, T.M., Wei, W., Potts, R., Ciochon, R., Kullmer, O., Schrenk, F.,

Hublin, J.-J., 2008. Molar enamel thickness and dentine horn height in *Gigantopithecus blacki*. Am. J. Phys. Anthropol. 135, 85-91.

Ortiz, A., Skinner, M.M., Bailey, S.E., Hublin, J.-J., 2012. Carabelli's trait revisited: n examination of mesiolingual features at the enamel-dentine junction and enamel surface of *Pan* and *Homo sapiens* upper molars. J. Hum. Evol. 63, 586-596.

Rink, W.J., Wei, W., Bekken, D., Jones, H.L., 2008. Geochronology of *Ailuropoda–Stegodon* fauna and *Gigantopithecus* in Guangxi Province, southern China. Quatern. Res. 69, 377-387.

Rohlf, F.J., 1998a. TpsDig2. Ecology and Evolution, SUNY. Stony Brook, New York. 32 http://life.bio.sunysb.edu/morph/.

Rohlf, F., 1998b. TpsRelw. Ecology and Evolution, SUNY. Stony Brook, New York. http://life.bio.sunysb.edu/morph/.

Scott, G.R., Turner, C.G., 1997. The Anthropology of Modern Human Teeth: Dental Morphology and its Variation in Recent Human Populations. Cambridge University Press, Cambridge.

Skinner, M.M., Gunz, P., Wood, B.A., Hublin, J.-J., 2008. Enamel-dentine junction (EDJ) morphology distinguishes the lower molars of *Australopithecus africanus* and *Paranthropus robustus*. J. Hum. Evol. 55, 979-988.

Skinner, M.M., Gunz, P., Wood, B.A., Boesch, C., Hublin, J.-J., 2009. Discrimination of extant *Pan* species and subspecies using the enamel–dentine junction morphology of lower molars. Am. J. Phys. Anthropol. 140, 234-243.

Skinner, M.M., Evans, A., Smith, T.M., Jernvall, J., Tafforeau, P., Kupczik, K., Olejniczak, A.J., Rosas, A., Radovčcic, J., Thackeray, J.F., Toussaint, M., Hublin, J.-J., 2010. Brief Communication: contributions of enamel-dentine junction shape and enamel deposition to primate molar crown complexity. Am. J. Phys. Anthropol. 142, 157-163.

Smith, T.M., Olejniczak, A.J., Martin, L.B., Reid, D.J., 2005. Variation in hominoid molar enamel thickness. J. Hum. Evol. 48, 575-592.

Smith, T.M., Olejniczak, A.J., Kupczik, K., Lazzari, V., Vos, J., Kullmer, O., Schrenk, F., Hublin, J.-J., Jacob, T., Tafforeau, P., 2009. Taxonomic assessment of the Trinil molars using non-destructive 3D structural and developmental analysis. PaleoAnthropol. 117-129.

Smith, T.M., Bacon, A.M., Demeter, F., Kullmer, O., Nguyen K.T., Vos, J., Wei, W., Zermeno, J.P., Zhao, L.X., 2011. Dental tissue proportions in fossil orangutans from mainland Asia and Indonesia. Hum. Origins Res. 1, 1-6.

Sun, C., Zhou, M., Xing, S., 2011. Geometric and morphometric analysis of Middle Pleistocene hominin teeth from Yiyuan, Shandong Province. Acta Anthropol. Sinica 30, 32-44.

Sun, C., Xing, S., Martín-Francés, L., Bae, C., Liu, L., Wei, G., Liu, W., 2014. Interproximal grooves on the Middle Pleistocene hominin teeth from Yiyuan, Shandong Province: New evidence for tooth-picking behavior from eastern China. Quatern. Int. 354, 162-168.

Suwa, G.E.N., Asfaw, B., Haile-Selassie, Y., White, T.I.M., Katoh, S., Woldegabriel, G., Hart, W.K., Nakaya, H., Beyene, Y., 2007. Early Pleistocene *Homo erectus* fossils from Konso, southern Ethiopia. Anthropol. Sci. 115, 133-151.

Tobias, P.V., 1991. Olduvai Gorge, volume 4: The skulls, endocasts and teeth of *Homo habilis*. Cambridge University Press, Cambridge.

Tobias, P.V., Koenigswald, G.H.R.V., 1964. A comparison between the Olduvai hominines and those of Java and some implications for hominid phylogeny. Nature 204, 515-518.

Turner, C.G., II, Nichol, C.R., Scott, G.R., 1991. Scoring procedures for key morphological traits of 33 the permanent dentition: the Arizona State University dental anthropology system. In: Kelley, M., Larsen, C. (Eds.), Advances in Dental Anthropology. Wiley-Liss, New York, pp. 13-31.

Tyler, D.E., 2003. Sangiran 5, ("*Pithecanthropus dubius*"), *Homo erectus,* "*Meganthropus,*" or *Pongo*? Hum. Evol. 18, 229-242.

Tyler, D.E., 2004. An examination of the taxonomic status of the fragmentary mandible Sangiran 5, (*Pithecanthropus dubius*), *Homo erectus,* "*Meganthropus*", or *Pongo*? Quatern. Int. 117, 125-130.

Ungar, P.S., Grine, F.E., Teaford, M.F. Perez-Perez, A., 2001. A review of interproximal wear grooves on fossil hominin teeth with new evidence from Olduvai Gorge. Archs. Oral Biol. 46, 285-292.

Walker, A., Leakey, R.E., 1993. The Nariokotome *Homo erectus* Skeleton. Harvard University Press,

Cambridge, MA.

Wang, C.-B., Zhao, L.-X., Jin, C.-Z., Wang, Y., Qin, D.-G., Pan, W.-S., 2014. New discovery of Early Pleistocene orangutan fossils from Sanhe Cave in Chongzuo, Guangxi, southern China. Quatern. Int. 354, 68-74.

Ward, S.C., Johanson, D.C., Coppens, Y., 1982. Subocclusal morphology and alveolar process relationships of hominid gnathic elements from the Hadar formation: 1974–1977 collections. Am. J. Phys. Anthropol. 57, 605-630.

Weidenreich, F., 1937. The dentition of *Sinanthropus pekinensis*: a comparative odontography of the hominids. Palaeont. Sinica D 1, 1-180.

White, T.D., 1980. Additional fossil hominids from Laetoli, Tanzania: 1976–1979 specimens. Am. J. Phys. Anthropol. 53, 487-504.

Wolpoff, M.H., 1971. Metric Trends in Hominid Dental Evolution. Case Western Reserve University Press, Cleveland.

Woo, J., Chia, L., 1954. New discoveries of *Sinanthropus pekinensis* in Choukoutien. Acta Palaeontol. Sinica 2, 267-288.

Wood, B., 1991. Hominid Cranial Remains. Koobi Fora Research Project, Vol. 4. Clarendon Press, Oxford.

Wood, B.A., Abbott, S.A., Graham, S.H., 1983. Analysis of the dental morphology of Plio-Pleistocene hominids: II. Mandibular molars-study of cusp areas, fissure pattern and cross sectional shape of the crown. J. Anat. 137, 287-314.

Wu, R., Wu, X., Huang, W., Qi, G., 1999. Paleolithic Sites in China. Shanghai Scientific and Technological Education Publishing House, Shanghai.

Wu, X., Poirier, F., 1995. Human Evolution in China. A Morphometric Description of Fossils and a Review of the Sites. Oxford University Press, New York.

Xing, S., 2012. Morphological variation of Zhoukoudian *Homo erectus* teeth. Ph.D. Dissertation,
34
Chinese Academy of Science.

Xing, S., Martinón-Torres, M., Bermúdez de Castro, J.M., Zhang, Y., Fan, X., Zheng, L., Huang, W., Liu, W., 2014. Middle Pleistocene hominin teeth from Longtan Cave, Hexian, China. PLoS ONE 9, e114265.

Xing, S., Martinón-Torres, M., Bermúdez de Castro, J.M., Wu, X., Liu, W., 2015. Hominin teeth from the early Late Pleistocene site of Xujiayao, Northern China. Am. J. Phys. Anthropol. 156, 224-240.

Xu, C., Zhang, Y., Chen, C., Fang, D., 1984. Human occipital bone and mammalian fossils from Chaoxian, Anhui. Acta Anthropol. Sinica 3, 202-209.

Zaim, Y., Ciochon, R.L., Polanski, J.M., Grine, F.E., Bettis, E.A. 3rd, Rizal, Y., Franciscus, R.G., Larick, R.R., Heizler, M., Aswan, Eaves, K.L., Marsh, H.E., 2011. New 1.5 million-year-old *Homo erectus* maxilla from Sangiran (Central Java, Indonesia). J. Hum. Evol. 61, 363-376.

Zanolli, C., 2013. Additional evidence for morpho-dimensional tooth crown variation in a new Indonesian *H. erectus* sample from the Sangiran Dome (Central Java). PLoS ONE 8, e67233.

Zanolli, C., 2015. Brief Communication: Molar crown inner structural organization in Javanese *Homo erectus*. Am. J. Phys. Anthropol. 156, 148-157.

Zanolli, C., Bayle, P., Macchiarelli, R., 2010. Tissue proportions and enamel thickness distribution in the early Middle Pleistocene human deciduous molars from Tighenif, Algeria. C. R. Palevol 9, 341-348.

Zanolli, C., Bondioli, L., Mancini, L., Mazurier, A., Widianto, H., Macchiarelli, R., 2012. Brief Communication: Two human fossil deciduous molars from the Sangiran Dome (Java, Indonesia): Outer and inner morphology. Am. J. Phys. Anthropol. 147, 472-481.

Zanolli, C., Bondioli, L., Coppa, A., Dean C.M., Bayle, P., Candilio, F., Capuani, S., Dreossi, D., Fiore, I., Frayer, D.W., Libsekal, Y., Mancini, L., Rook, L., Medin Tekle, T., Tuniz, C., Macchiarelli, R., 2014. The late Early Pleistocene human dental remains from Uadi Aalad and Mulhuli-Amo (Buia), Eritrean Danakil: Macromorphology and microstructure. J. Hum. Evol. 74, 96-113.

Zanolli, C., Grine, F.E., Kullmer, O., Schrenk, F., Macchiarelli, R., 2015. The early Pleistocene deciduous hominid molar FS-72 from the Sangiran Dome of Java, Indonesia: A taxonomic reappraisal based on its comparative endostructural characterization. Am. J. Phys. Anthropol. DOI: 10.1002/ajpa.22748.

Zelditch, M.L., Swiderski, D.L., Sheets, H.D., Fink, W.L., 2004. Geometric Morphometrics for Biologists: A Primer. Elsevier Academic Press, San Diego.

Zhang, Y., Liu, W., 2002. Dental morphological distinctions between *Homo erectus* and early *Homo sapiens* in China. Acta Anthropol. Sinica 21, 87-101.

Zhao, L., Wang, C., Jin, C., Qin, D., Pan, W., 2009. Fossil orangutan-like hominoid teeth from
35
Late Pleistocene human site of Mulanshan cave in Chongzuo of Guangxi and implications on taxonomy and evolution of orangutan. Chin. Sci. Bull. 54, 3924-3930.
36

Figure legends

Figure 1. The geographic location of Yiyuan compared to other major Chinese sites, and the stratigraphic sequences (upper left) of Localities 1 and 3 of Yiyuan site (after Lu et al., 1989). From top to bottom, Locality 1 comprises: brownish silty clay, $50 - 60$ cm thick, in Layer 1; brownish red clay ($55 - 85$ cm thick) containing a few calcareous concretions with irregular shapes in Layer 2; reddish brown silty clay ($15 - 40$ cm thick) in Layer 3, in which the hominin skull, two isolated teeth (Sh.y.005, 007), and abundant faunal remains were found; brownish red silty clay ($30 - 55$ cm thick) in Layer 4, which starts from a calcareous bed 10 cm thick and includes limestone breccia, a quartz cube, and petrosilex fragments; dark brown and brownish red sand overlain by a thin calcareous bed ($90 - 130$ cm thick) in Layer 5, with the main component of the brownish red sand being a plentiful round breccia, in addition to a few breccia and mammal fossils found in the upper dark brown sand (Lu et al., 1989). From top to bottom, Locality 3 comprises: brownish silty clay ($15 - 50$ cm thick) in Layer 1; brownish yellow clay ($35 - 45$ cm thick) in Layer 2; dark brown silty clay containing a few calcareous concretions, breccia, and manganese nodules (190 cm thick) in Layer 3, which yielded five isolated hominin teeth (Sh.y.003, 004, 008, 071, and 072), as well as abundant faunal remains; brownish clay (100 cm thick) in Layer 4, from which a few mammal fossils was recovered; brownish yellow sand (120 cm thick), including a breccia and gravel mainly made of quartz, in Layer 5 (Lu et al., 1989). The images and descriptions of stratigraphic sequences were based upon Lu, Z., Huang, W., Meng, Z. (1989). These materials were used with the permission from Acta Anthropologica Sinica.

Figure 2. The measurement of RDHH based on the 2D mesial sectional plane of Yiyuan M_2 (Y: the dentine horn height which is defined as the perpendicular distance from the dentine horn to the line parallel to the bi-cervical diameter and coursing through the lowest point of enamel in the mid-occlusal basin. X+Y: the total height of the dentine crown which is measured as the perpendicular distance from the dentine horn to the bi-cervical diameter). B: buccal; L: lingual.

Figure 3. Illustration of the landmarks (circles) and semi-landmarks (squares) chosen in the GM analyses of the occlusal surfaces of premolars (I), M_2 (II), C_1 (III), and M_2 (IV). D: distal, L: lingual.

Figure 4. Sh.y.003, 004, 007, and 071 from the Yiyuan site. All teeth are aligned in a similar fashion (from left to right: occlusal, buccal, mesial, lingual, and distal). B: buccal; M: mesial; D: distal.

Figure 5. The EDJ surfaces of Yiyuan teeth obtained from micro-CT scanning. The images are not scaled.
37

Figure 6. Sh.y.008, 005, and 072 from Yiyuan. All teeth are aligned in a similar fashion (from left to right: occlusal, labial or buccal, mesial, lingual, and distal). B: buccal; La: labial; M: mesial; D: distal.

Figure 7. Mesiodistal (upper row) and buccolingual (lower row) dimensions of the Yiyuan and *Pongo* teeth. Outliers are indicated by circles. Yiyuan values are represented by a single band on each plot.

Figure 8. Geometric morphometric analyses of P_3, P_4, M_2, C_1, and M_2 (TPS-grids correspond to the positive-value or negative-value extremes of the RW axis). All fossil hominins and recent modern humans are combined into a large comparative group. B: buccal; D: distal; M: mesial.

Figure 9. Morphological comparisons between the Yiyuan C_1 and comparative specimens (I: Yiyuan Sh.y.005; II: *Australopithecus africanus* Stw 222; III: Dmanisi D2678; IV: Atapuerca SH AT-276; V: recent modern humans; VI: fossil *Pongo*). L: lingual; M: mesial. The Stw 222 and AT-276 are originally left lower canines, and have been mirror-imaged using Adobe Photoshop® to facilitate their comparisons with the Yiyuan tooth.

Figure 10. Comparison of M_2 (upper row) and M_2 (lower row) dentine surfaces of Yiyuan, Hexian, Zhoukoudian and *Pongo* teeth (the Zhoukoudian, Hexian, and *Pongo* specimens were mirror-imaged to facilitate the comparison with the Yiyuan M_2).

Figure 11. Geometric morphometric analyses of P_3 crown outline shapes and the position of anterior and posterior foveae (TPS-grids correspond to the positive-value or negative-value extremes of the

RW axis). B: buccal; M: mesial.

Figure 12. Geometric morphometric analyses of P$_4$ crown outline shapes and the position of anterior and posterior foveae (TPS-grids correspond to the positive-value or negative-value extremes of the RW axis). B: buccal; D: distal.

Figure 13. Measurement of relative cuspal areas of the Yiyuan M$_2$ and comparative specimens (YY: Yiyuan; AUS: *Australopithecus*; AEH: African Early *Homo*; HER: *H. ergaster*; NAMP: North African Middle Pleistocene; EAEP: East Asian Early Pleistocene; EAmMP: East Asian mid-Middle Pleistocene; EAlMP: East Asian late Middle Pleistocene; EALP: East Asian Late Pleistocene; WAEP: West Asian Early Pleistocene; WALP: West Asian Late Pleistocene; EEP: European Early Pleistocene; EMP: European Middle Pleistocene; NEA: Neanderthal; ELP: European Late Pleistocene; RMH: Recent modern humans). Outliers are indicated by circles. Groups represented by a single individual 38

are represented by a single band. A line corresponding to the Yiyuan value extends horizontally across each plot to facilitate visual comparisons.

Figure 14. Geometric morphometric analyses of M$_2$ crown outline shapes and the orientation of occlusal grooves (TPS-grids correspond to the positive-value or negative-value extremes of the relative warp [RW] axis). B: buccal; M: mesial.

Table 1. Fossil hominin teeth from the Yiyuan site.

Specimen No.	Tooth category	Individual	Crown measurements (mm)		Occlusal wear score
			MD	BL	
Sh.y.003	Upper right third premolar (RP^3)	I	8.6(8.7)	12.4	3
Sh.y.004	Upper left third premolar (LP^3)	I	8.7	12.4	3
Sh.y.005	Lower right canine (RC$_1$)	II	7.8(7.9)	8.4	4
Sh.y.007	Upper left second premolar (LP^4)	II	7.7(7.9)	11.2	4
Sh.y.008	Upper right second molar (RM^2)	I	11.4(11.6)	14.3	2
Sh.y.071	Upper left second premolar (LP^4)	I	8.2	12.3	3
Sh.y.072	Lower right second molar (RM$_2$)	III	10.9(11.1)	12.0	4

*The crown measurements in the parentheses are corrected values for the interproximal wear. MD: mesiodistal dimension, BL: buccolingual dimension.

Table 2. Specimens used in the metric and morphological comparisons.

Geography/ Chronology	Specimens	Sources of metrics
Africa		
Pliocene (*Australopithecus*)	Hadar, Laetoli, Makapansgat*, Sterkfontein*	1, 13
Late Pliocene and Early Pleistocene (Early *Homo*)	East Rudolf*, Olduvai, Omo Valley, Sterkfontein*	1, 13, 14, 20
Late Pliocene and Early Pleistocene (*H. ergaster*)**	East Rudolf*, West Turkana*	1, 17, 20

North African Middle Pleistocene	Rabat, Sidi Abderrhaman, Ternifine*, Thomas Quarry	1, 2

East Asia

Pongo pygmaeus	Guangxi*	This study
Early Pleistocene	Jianshi*, Sangiran*	3, 7, 8, 9, 15, 16, 23
Mid-Middle Pleistocene	Hexian*, Zhoukoudian (ZKD) Locality 1***	18, 19, 21
Late Middle Pleistocene	Chaoxian*, Panxian Dadong*, Xujiayao*	4, 10, 23
Early modern human	Liujiang*, Zhiren Cave*, Zhoukoudian (ZKD) Upper Cave	1
Holocene (Recent modern human)	Henan Province*, Hubei Province*	This study

West Asia

Early Pleistocene	Dmanisi*	11
Early modern human	Qafzeh*, Skhul	1

Europe

Early Pleistocene	Atapuerca-TD6*	5, 6
Middle Pleistocene	Arago*, Atapuerca SH*, Mauer, Montmaurin*, Petralona, Steinheim	1, 12
Neanderthals	Amud, Arcy Grotte Renne*, Arcy Hyene*, Arcy sur Cure (Mousterian), Chateauneuf, Ehringsdorf, Genay (Côte d'Or), Gibraltar, Hortus*, Krapina, Kulna, La Chaise, La Ferrassie, La Quina*, Monsempron*, Le Moustier, Ochoz, Petit Puymoyen*, Regourdou*, Saccopastore*, Sakajia, Shanidar, Spy, St. Césaire, Subalyuk, Tabun, Vindija	1
Early modern human	Abri Pataud*, Brno, Combe Capelle, Dolní Věstonice*, Cro-Magnon, Isturitz*, Le Rois*, Les Vachons, Mladeč, Pavlov*, Predmostí, Saint Germain-La Riviere*, Zlaty Kun	1

Note: "*" means that we examined the original fossils. For the rest, we employed high resolution casts.

1: contributed by Wolpoff; 2: Arambourg and Biberson, 1956; 3: Arif et al., 2002; 4: Bailey and Liu, 2010; 5: Bermúdez de Castro et al., 1999; 6: Carbonell et al., 2005; 7: Grine and Franzen, 1994; 8: Jacob, 1973; 9: Kaifu et al., 2005; 10: Liu et al., 2013; 11: Martinón-Torres et al., 2008; 12: Martinón-Torres et al., 2012; 13: Moggi-Cecchi et al., 2006; 14: Tobias, 1991; 15: Tobias and von Koenigswald, 1964; 16: Tyler, 2004; 17: Walker and Leakey, 1993; 18: Weidenreich, 1937; 19: Woo and Chia, 1954; 20: Wood, 1991; 21: Xing et al., 2014; 23: Xing et al., 2015; 24: Zaim et al., 2011.

** For some authors: African *H. erectus*

*** Three of the Zhoukoudian specimens are original fossils found in excavations of 1949-1951 and 1953. See Woo and Chia (1954) for more details.

Table 3. Relative dentine horn height (RDHH) of the paracone and the protocone of Yiyuan M^2 and comparative samples.

Data source	Paracone(%)		Protocone(%)	
	1	2	1	2
Yiyuan	37.4	-	35.5	-
Pongo	27.9(17.8-37.6)	27.1	23.9(18.6-31.4)	28.2
Recent Modern Human	39.7(30.2-50.7)	36.2	36.6(29.0-48.9)	35.3

*1: the present study; 2: Olejniczak et al. (2008)

Table 4. Summary of features presented in the text that differentiate or support the human versus *Pongo* nature of the Yiyuan teeth.

Individual	Specimen	Geography	Tooth-picking	Crown size	RDHH	GM	Descriptive Morphology
I	Sh.y.003 (P^3)	Yes	Yes	Yes	-	Yes	-
	Sh.y.004 (P^3)	Yes	Yes	Yes	-	Yes	-
	Sh.y.071 (P^4)	Yes	No	Yes	-	Yes	-
	Sh.y.008 (M^2)	Yes	Yes	No	Yes	No	Yes
II	Sh.y.005 (C_1)	Yes	No	Yes	-	Yes	Yes
	Sh.y.007 (P^4)	Yes	Yes	Yes	-	Yes	-
III	Sh.y.072 (M_2)	Yes	Yes	Yes	-	Yes	Yes

*"-" means missing value.
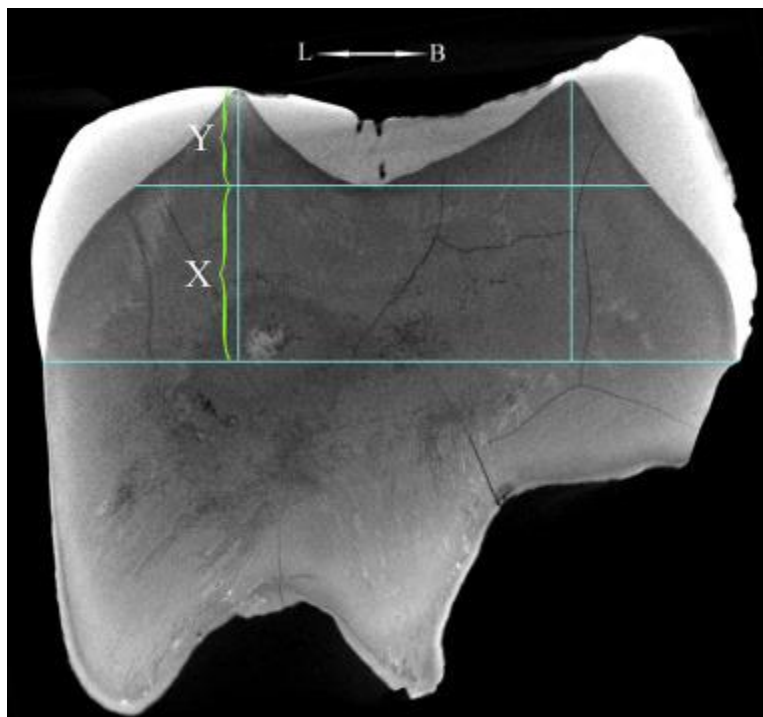
Figure 1

Figure 2

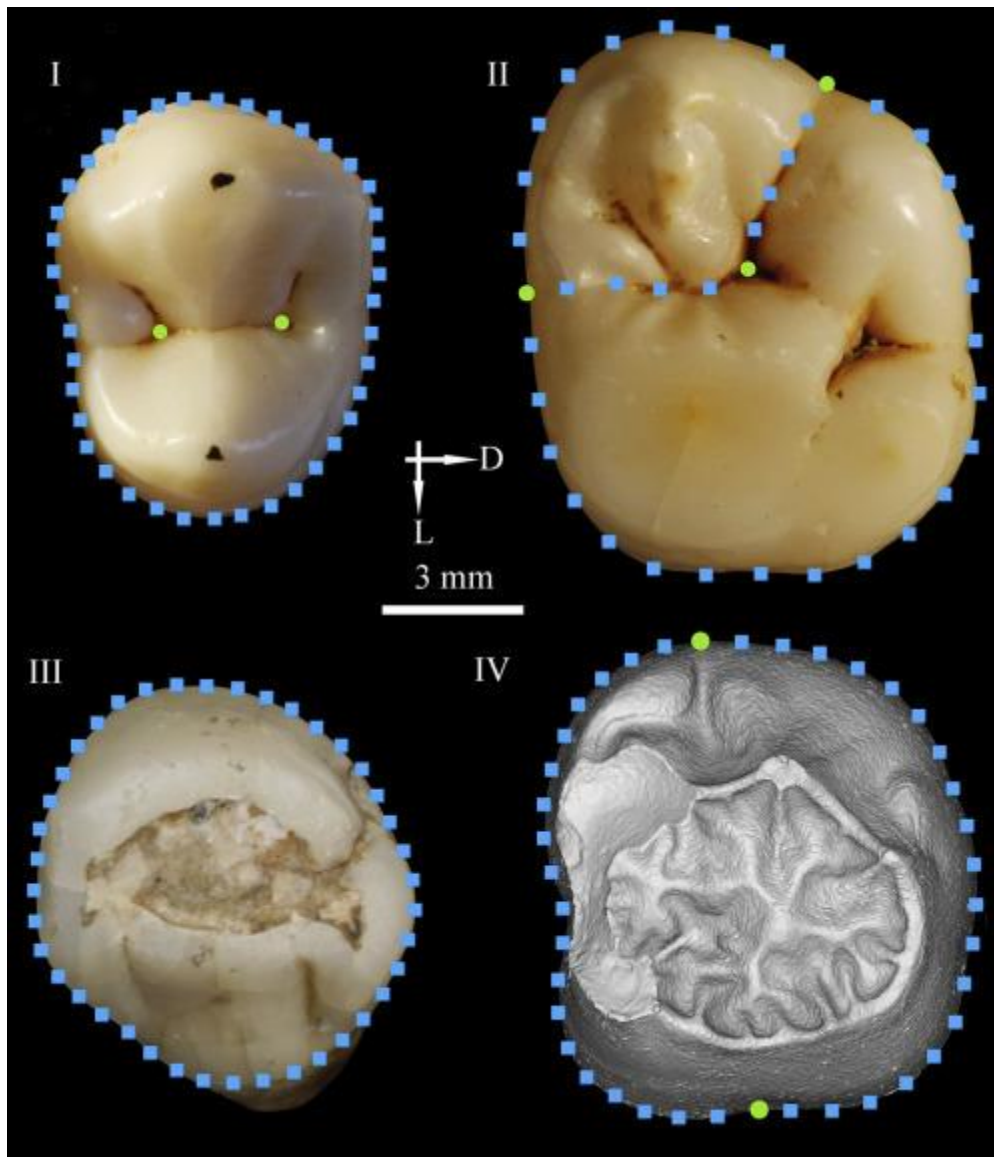Figure 3

Figure 4

Figure 5

Sh.y.003   Sh.y.004   Sh.y.007   Sh.y.071

Sh.y.008   Sh.y.005   Sh.y.072

Figure 6

Figure 7

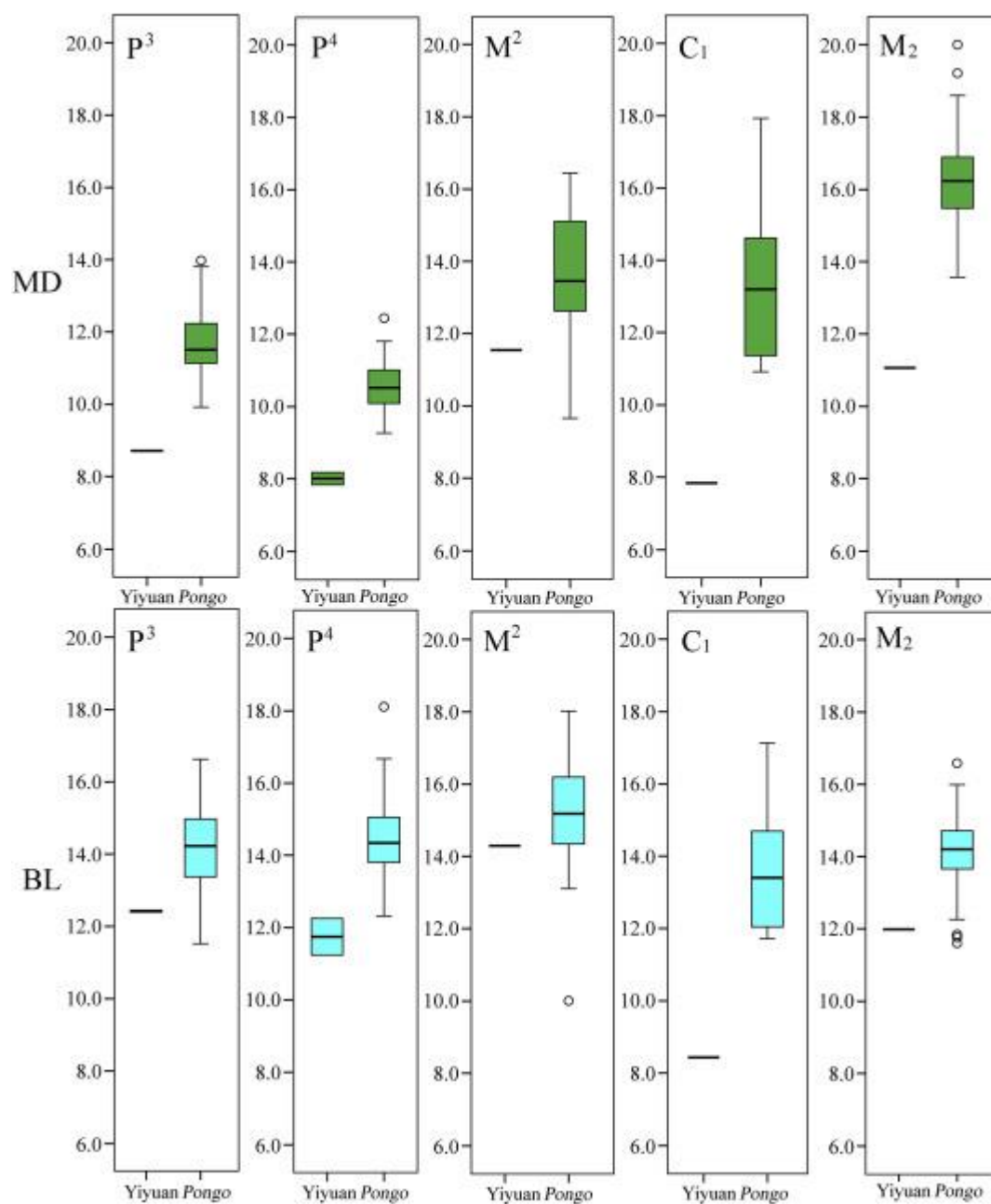Figure 8

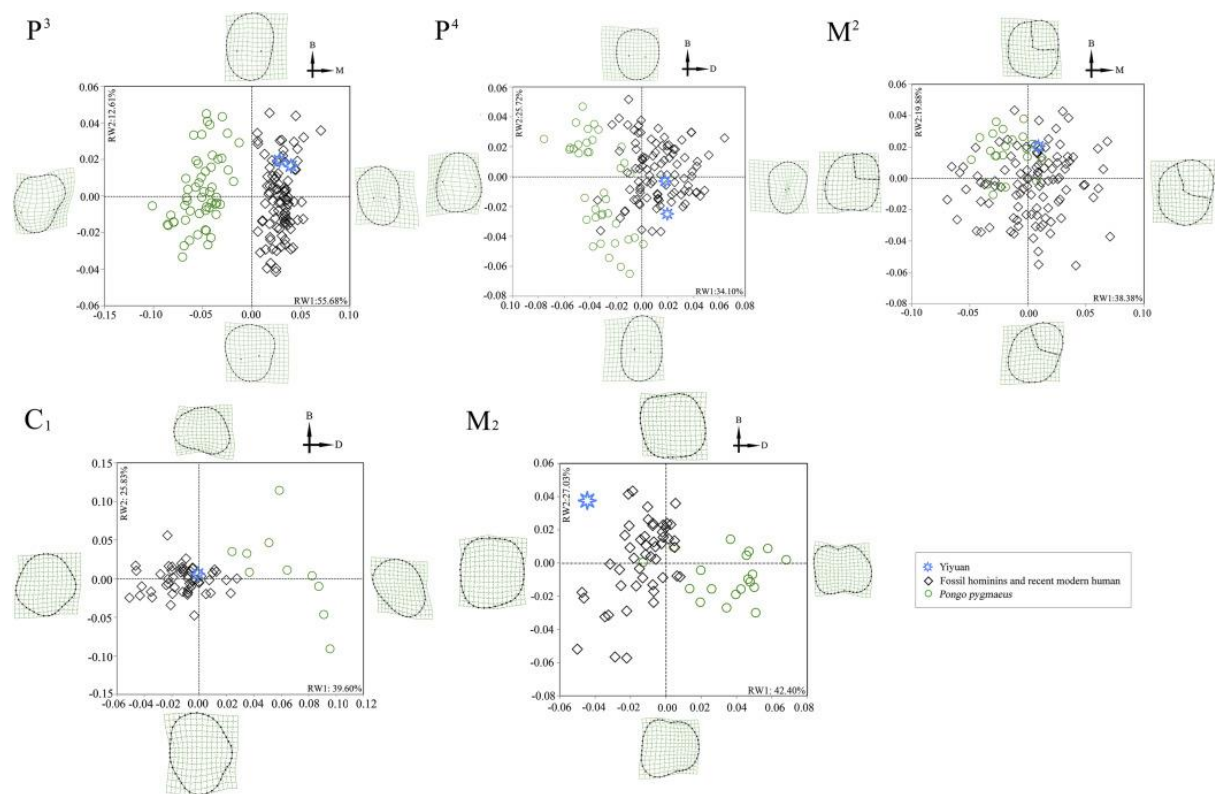Figure 9

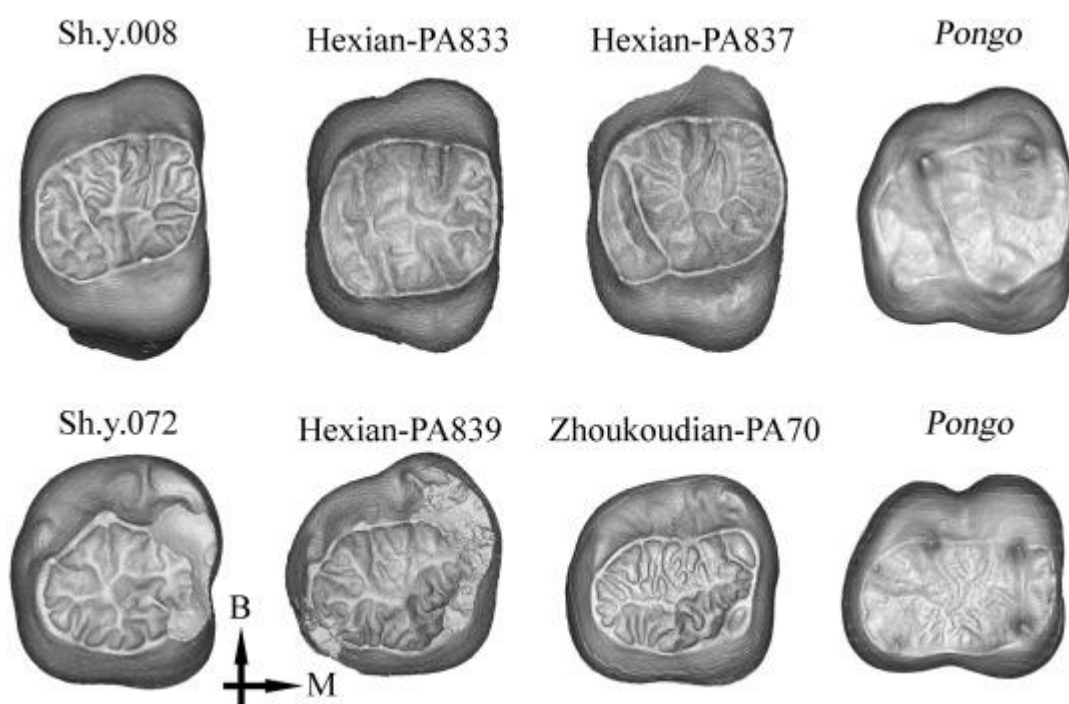Figure 10
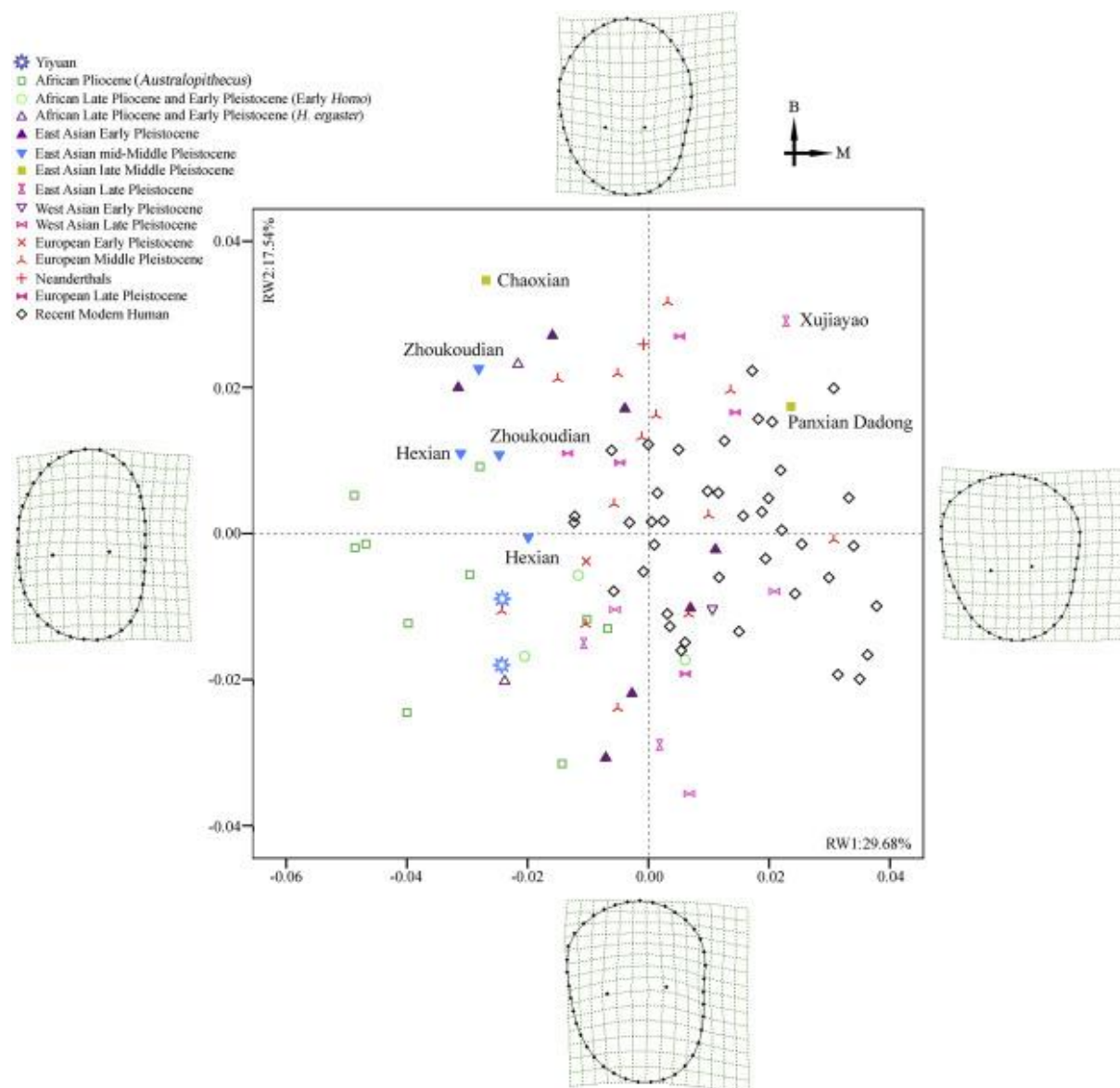
Sh.y.008   Hexian-PA833   Hexian-PA837   *Pongo*

Sh.y.072   Hexian-PA839   Zhoukoudian-PA70   *Pongo*
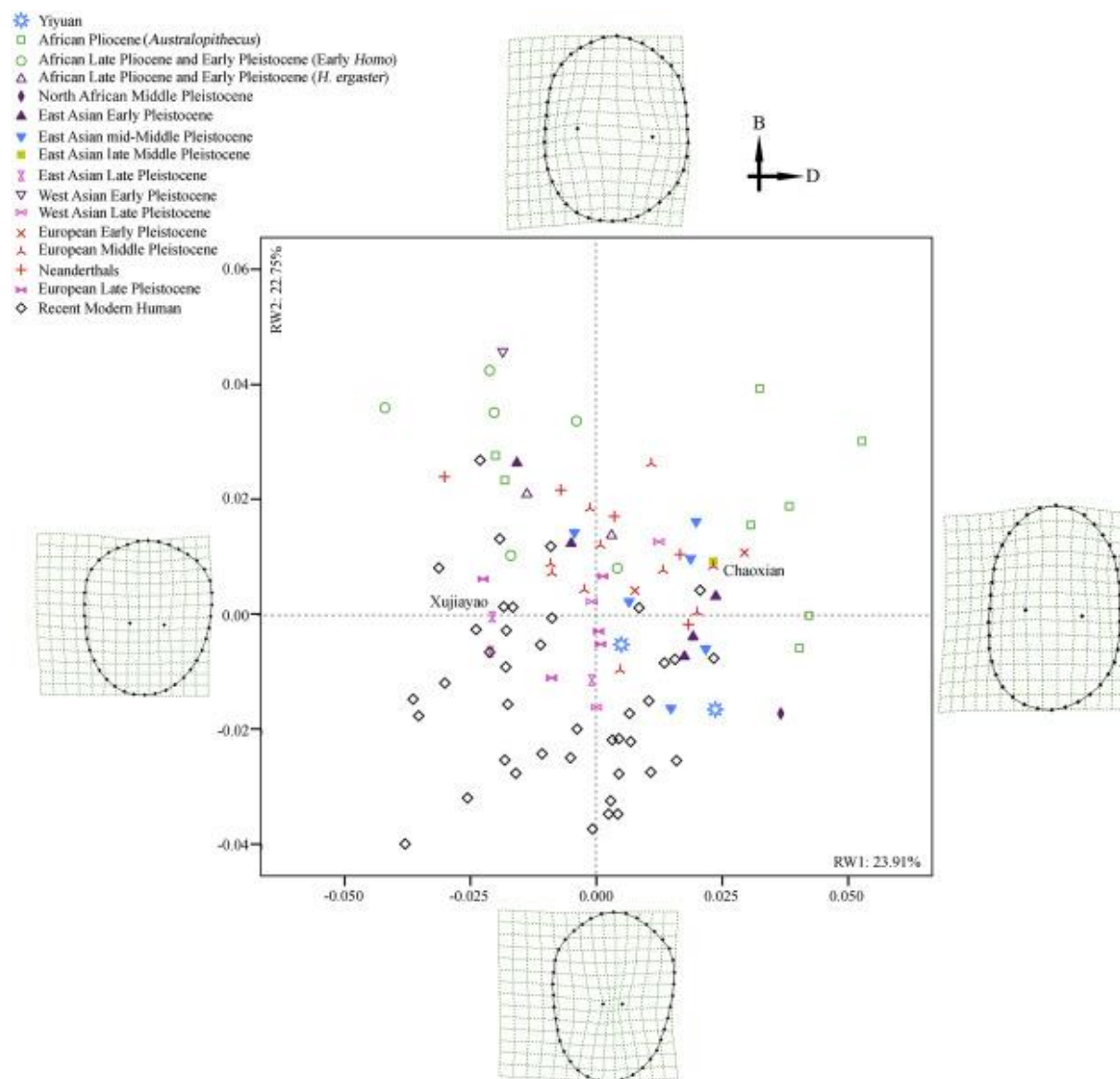
Figure 11

Figure 12

Figure 13

Figure 14

Legend (left side):
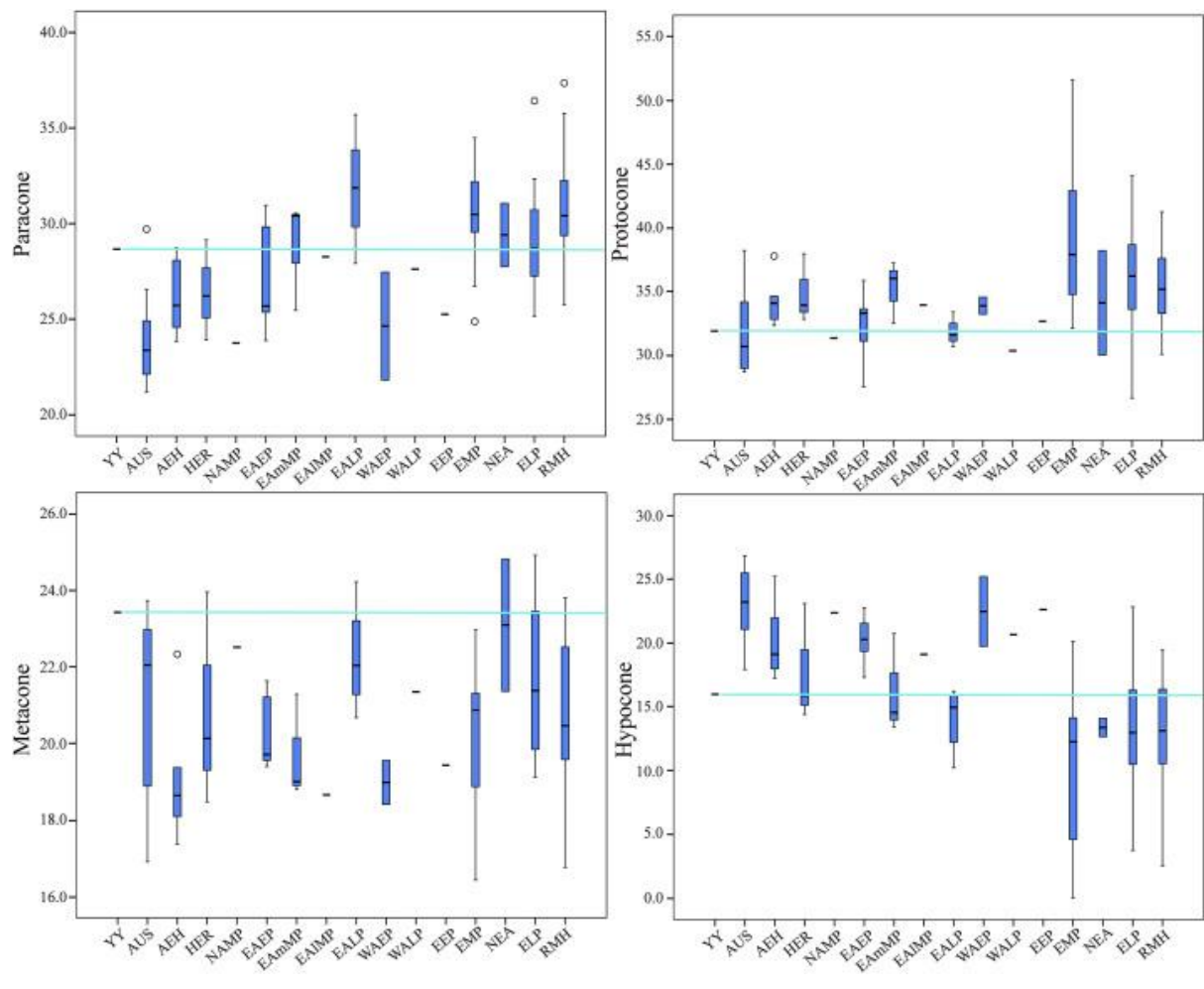- Yiyuan
- African Pliocene (*Australopithecus*)
- African Late Pliocene and Early Pleistocene (Early *Homo*)
- African Late Pliocene and Early Pleistocene (*H. ergaster*)
- North African Middle Pleistocene
- East Asian Early Pleistocene
- East Asian mid-Middle Pleistocene
- East Asian late Middle Pleistocene
- East Asian Late Pleistocene
- West Asian Early Pleistocene
- West Asian Late Pleistocene
- European Early Pleistocene
- European Middle Pleistocene
- Neanderthals
- European Late Pleistocene
- Recent Modern Human

Axis labels: RW2: 19.50%, RW1: 40.51%

Plot labels: Hexian, Hexian, Xujiayao, Chaoxian

B, M